Lawrence Berkeley National Laboratory
Recent Work

Title

A nn PHASE SHIFT ANALYSIS FROM REACTIONS n+p->n+n-A++ AND n+p ->K+K- A++ AT 7. 1 GeV/c.

Permalink
https://escholarship.org/uc/item/0v92m7m9

Author
Protopopescu, S.D.

Publication Date
1972-04-01

eScholarship.org Powered by the California Digital Library
University of California

Presented at Intern. Conf. on
Meson Spectroscopy, Philadelphia,
Pa., April 28-29, 1972

LBL-787 Rev.
Preprint

A $\pi\pi$ PHASE SHIFT ANALYSIS FROM REACTIONS $\pi^+ p \to \pi^+ \pi^- \Delta^{++}$ AND $\pi^+ p \to K^+ K^- \Delta^{++}$ AT 7.1 GeV/c

S. D. Protopopescu, M. Alston-Garnjost, A. Barbaro-Galtieri,
S. M. Flatté, J. H. Friedman, T. A. Lasinski, G. R. Lynch,
M. S. Rabin, and F. T. Solmitz

April 1972

AEC Contract No. W-7405-eng-48

For Reference

Not to be taken from this room

LBL-787

DISCLAIMER

This document was prepared as an account of work sponsored by the United States Government. While this document is believed to contain correct information, neither the United States Government nor any agency thereof, nor the Regents of the University of California, nor any of their employees, makes any warranty, express or implied, or assumes any legal responsibility for the accuracy, completeness, or usefulness of any information, apparatus, product, or process disclosed, or represents that its use would not infringe privately owned rights. Reference herein to any specific commercial product, process, or service by its trade name, trademark, manufacturer, or otherwise, does not necessarily constitute or imply its endorsement, recommendation, or favoring by the United States Government or any agency thereof, or the Regents of the University of California. The views and opinions of authors expressed herein do not necessarily state or reflect those of the United States Government or any agency thereof or the Regents of the University of California.

0 0 0 0 3 8 0 0 2 3 9

A ππ PHASE SHIFT ANALYSIS FROM REACTIONS $\pi^+ p \to \pi^+ \pi^- \Delta^{++}$ AND $\pi^+ p \to K^+ K^- \Delta^{++}$ AT 7.1 GeV/c*†

S. D. Protopopescu, M. Alston-Garnjost, A. Barbaro-Galtieri, S. M. Flatté, J. H. Friedman, T. A. Lasinski, G. R. Lynch, M. S. Rabin, and F. T. Solmitz

Lawrence Berkeley Laboratory, University of California
Berkeley, California 94720

April 1972

ABSTRACT

We present results of an energy-dependent ππ phase shift analysis for ππ energies between 550 and 1150 MeV. The $I = 0$ s wave is parametrized in term of a 2×2 M-matrix coupling ππ and KK channels. A unique solution is obtained for this wave.

I. INTRODUCTION

Most of the information on ππ phase shifts so far has come from reactions of the form $\pi N \to \pi\pi N$.[1] Extrapolations to the π pole using this reaction suffer from the fact that the amplitudes contain a kinematical zero somewhere between $t_{NN} = \mu^2$ (π-mass squared) and $t_{NN} = 0$. Because of absorption effects the position of this zero is not known with precision and may occur at different values of t_{NN} for each partial wave amplitude. This makes results of extrapolations uncertain. Reactions of the form $\pi N \to \pi\pi\,\Delta$ do not have this problem, therefore one can extrapolate the normalized Y_L^0 moments. In addition, one can check the validity of the extrapolation by comparing the extrapolated Y_L^0 moments of the $\pi^+ p$ vertex with the moments for physical $\pi^+ p$ scattering. These advantages are partially offset by the fact that $|t_{N\Delta}|_{min}$ (minimum momentum transferred squared) is larger, requiring an extrapolation over a larger interval of $t_{N\Delta}$. Because of these problems a detailed analysis from a single experiment cannot be expected to give definitive values for the phases and inelasticities. In the absence of physical ππ scattering one can only hope that a consistent set of solutions may emerge from various different reactions at different energies.

We will present here results of a ππ phase shift analysis using the reactions:

---

*Work done under the auspices of the U. S. Atomic Energy Commission.

† A more detailed version of this paper will be submitted to Phys. Rev.

1) $\pi^+ p \to \pi^+\pi^- \Delta^{++}$ (32 100 events, $|t_{p\Delta}| < 0.4$ GeV^2)

(data extrapolated to π - pole),

2) $\pi^+ p \to K^+K^- \Delta^{++}$ (682 events, $|t'_{p\Delta}| = |t - t_{min}| \leq 0.1$ GeV^2)

at an incident beam momentum of 7.1 GeV/c^2.

The $\pi^+\pi^- \to \pi^+\pi^-$ cross section was obtained by a Chew-Low linear extrapolation in $t_{p\Delta}$ modified by Dürr-Pilkuhn form factors. The Y^0_L moments were obtained by a simple linear extrapolation in $t_{p\Delta}$. To extract phases and inelasticities, energy-dependent fits were done to the cross section and Y^0_L moments (up to L = 6) between 550 and 1150 MeV. The I (isospin) = 2 amplitudes were assumed to be elastic everywhere, the L $\neq$ 0 (I $\neq$ 2) were allowed to become inelastic at the $\omega\pi$ threshold ($\sim$900 MeV). The I = 0 s wave was described by a 2$\times$2 M-matrix which coupled $\pi\pi$ and $\bar{K}K$ channels. The phase (δ^0_0) obtained for the s wave rules out the "up" solution (narrow ϵ) and varies rapidly before the $\bar{K}K$ threshold ($\delta_0^0 = 90°$ at $\sim$900 MeV, $\delta_0^0 = 180°$ at $\sim$990 MeV).

All the fits with reasonable χ^2 gave essentially the same phases and inelasticities within the computed errors. Using the M-matrix parametrization, we looked for poles in the I = 0 s-wave amplitude. We always found one pole (S*) on the second Riemann sheet at 980 ± 6 -i (37 ± 8) which can be interpreted as a $K\bar{K}$ bound state. We believe the evidence for this pole to be conclusive. We also found another pole which could be either on the second Riemann sheet at 600 ± 100 -i (250 ± 70) or on the fourth Riemann sheet at 650 ± 70 -i (150 ± 50). In either case this pole is very far from the physical region and considerably more data are probably needed to determine on which sheet it is. Also, the effect of the 4π cut (which we neglect) might have to be included.

The higher waves are less well determined above 900 MeV; the data require some of these waves to be very inelastic, but without more information from other channels it is difficult to choose among the various possibilities. In addition, there are some indications that the simple linear extrapolation does not successfully remove non-π-exchange background. A smooth background will not affect the s-wave results very much since they depend on the very sharp structure in the data, but can severely distort results on those partial waves which are assumed to be slowly varying.

II. EXPERIMENTAL DATA

Our experiment is a 700 000-picture exposure (42 ± 1.2 events/μb) of the SLAC 82-inch bubble chamber to an rf-separated π^+ beam at 7.1 GeV/c. We observe 420 000 four-prongs, of which 72 700 fit the hypothesis $\pi^+ p \to \pi^+\pi^-\pi^+ p$ and 4600 fit $\pi^+ p \to K^+K^-\pi^+ p$. After correcting for scanning and measuring efficiencies the effective path length for the above sample of events is 39 ± 1 events/μb. The error on the cross section is larger for K^+K^- events because about 10% of these are ambiguous with $\pi^+\pi^-$ events.

For the extrapolation we use only events with $|t_{p\Delta}| < 0.4$ GeV^2, where the Δ^{++} is defined as the π^+p combination with $1.13 < M(\pi^+p) <$ 1.36 GeV. After the selection we are left with 32 100 $\pi^+\pi^-\ \Delta^{++}$ events. Of these about 5% are ambiguous, having two Δ^{++} by our definition; in case of ambiguity, the π^+p combination with smaller $|t_{p\Delta}|$ was chosen as the Δ^{++}. From the mass and t distributions for ambiguous events we estimate that no more than 300 events may be misinterpreted (or may be double Δ^{++} events). Figure 1 shows the data before and after the selections. The mass resolution for $\pi^+\pi^-$ events varies somewhat as a function of mass, being ±5 MeV in the ρ region (760 MeV) and ±8 MeV in the f_0 region; the dependence on ππ angles is generally small. For further details on the mass resolution see Ref. 2.

The mass distribution and spherical harmonic moments of the $\pi^+\pi^-$ system are shown in Fig. 2. We present the extrapolated data and the data for $|t'_{p\Delta}| < 0.1$ GeV^2 in the same binning for comparison. To calculate the $K\bar{K}$ cross section we simply took the ratio of K^+K^- events to $\pi^+\pi^-$ events for $|t'_{p\Delta}| < 0.1$ GeV^2 and multiplied by twice the ππ extrapolated cross section (the first bin has a small correction to account for the mass difference between K^+ and K^0). Note that, except for the magnitude, the general behavior of the extrapolated moments is not very different from the one observed in the physical region. The only noteworthy exception is Y_3^0, which stays close to zero below 1.1 GeV instead of being negative. The most striking feature of the data is the sharp structure in Y_1^0, Y_2^0 and the $\pi^+\pi^-$ cross section near 980 MeV. The Y_1^0 moment drops from 0.16 to 0 between 980 and 990 MeV [the data for $|t'_{p\Delta}| < 0.1$ (GeV)^2 was published in 10-MeV bins in Ref. 3]; Y_2^0 has a sharp rise before 980 MeV; and the mass distribution has a shoulder between 910 and 950 MeV, a rapid drop between 950 and 980 MeV, and is flat after 980 MeV. The simplest explanation for these effects is that we are observing a rapid change in the s wave associated with $K\bar{K}$ threshold.[3] A qualitative conclusion one can draw is that the s wave amplitude must be large around 930 MeV and both I = 0 and I = 2 s wave amplitude must be close to zero near the $K\bar{K}$ threshold.[4] The $K\bar{K}$ cross section rises sharply at threshold. As shown in Ref. 3, the charged 4π channel has essentially no events below 1.0 GeV and very few below 1.2 GeV. On the other hand, the $\pi^+\pi^-$ MM (missing mass MM $\geq 2\pi^0$) channel has substantially more events below 1 GeV but less than the $K\bar{K}$ channel, and the rise is more gentle starting around 900 MeV. If we believe π exchange is the major contribution to these channels then the difference between the charged 4π and the $\pi^+\pi^-$ MM mass distributions is easy to explain in terms of the ωπ channel which can only contribute to the second distribution. Information from these inelastic channels is not used explicitly in the phase shift analysis (except the $K\bar{K}$ cross section), but they

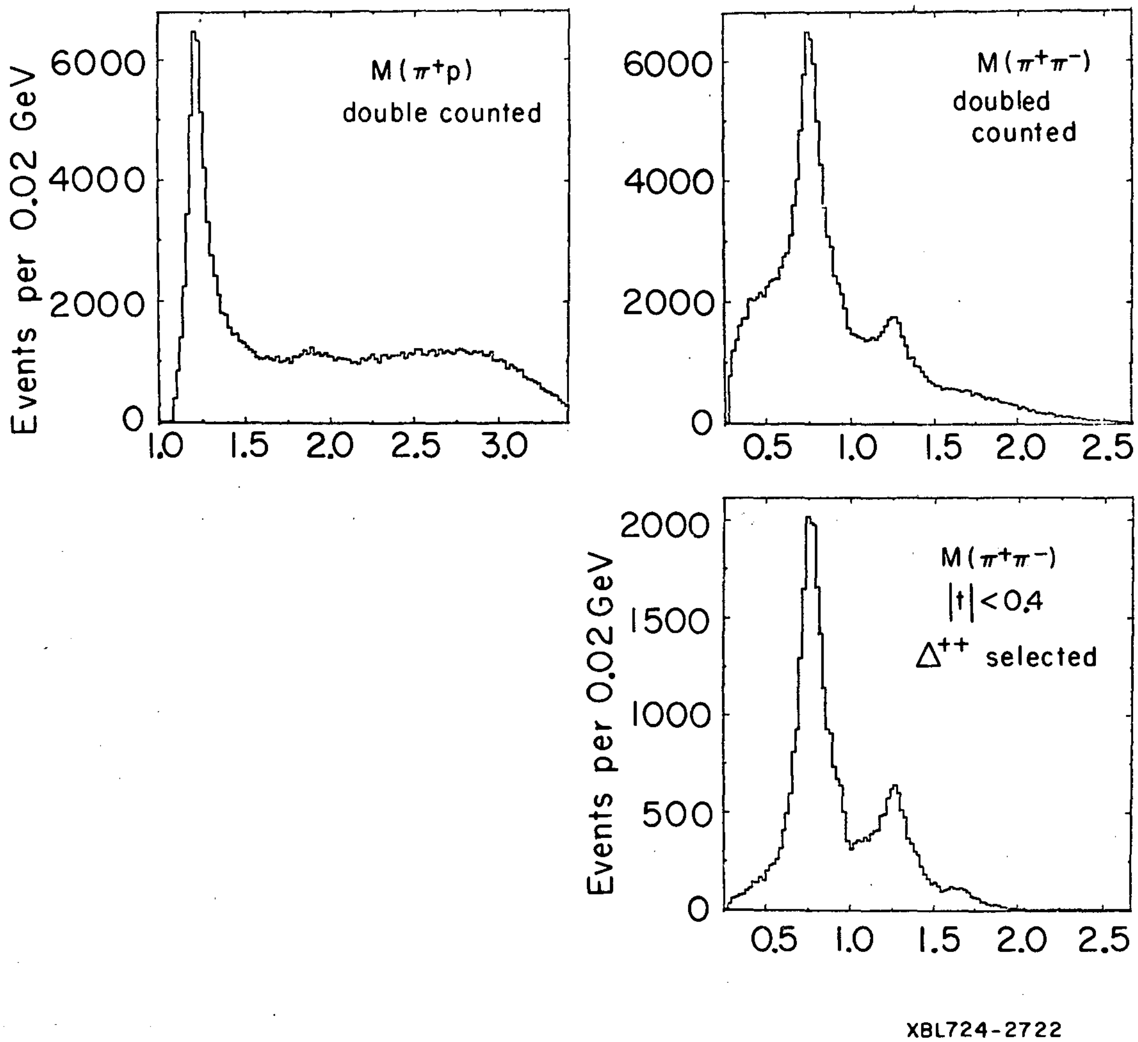

Fig. 1.(a) π^+p mass distribution in 20-MeV bins, both combinations included. (b) $\pi^+\pi^-$ mass distribution in 20-MeV bins, both combinations included. (c) $\pi^+\pi^-$ mass distribution in 20-MeV bins, Δ^{++} selected.

0 0 0 0 3 8 0 0 2 4 1

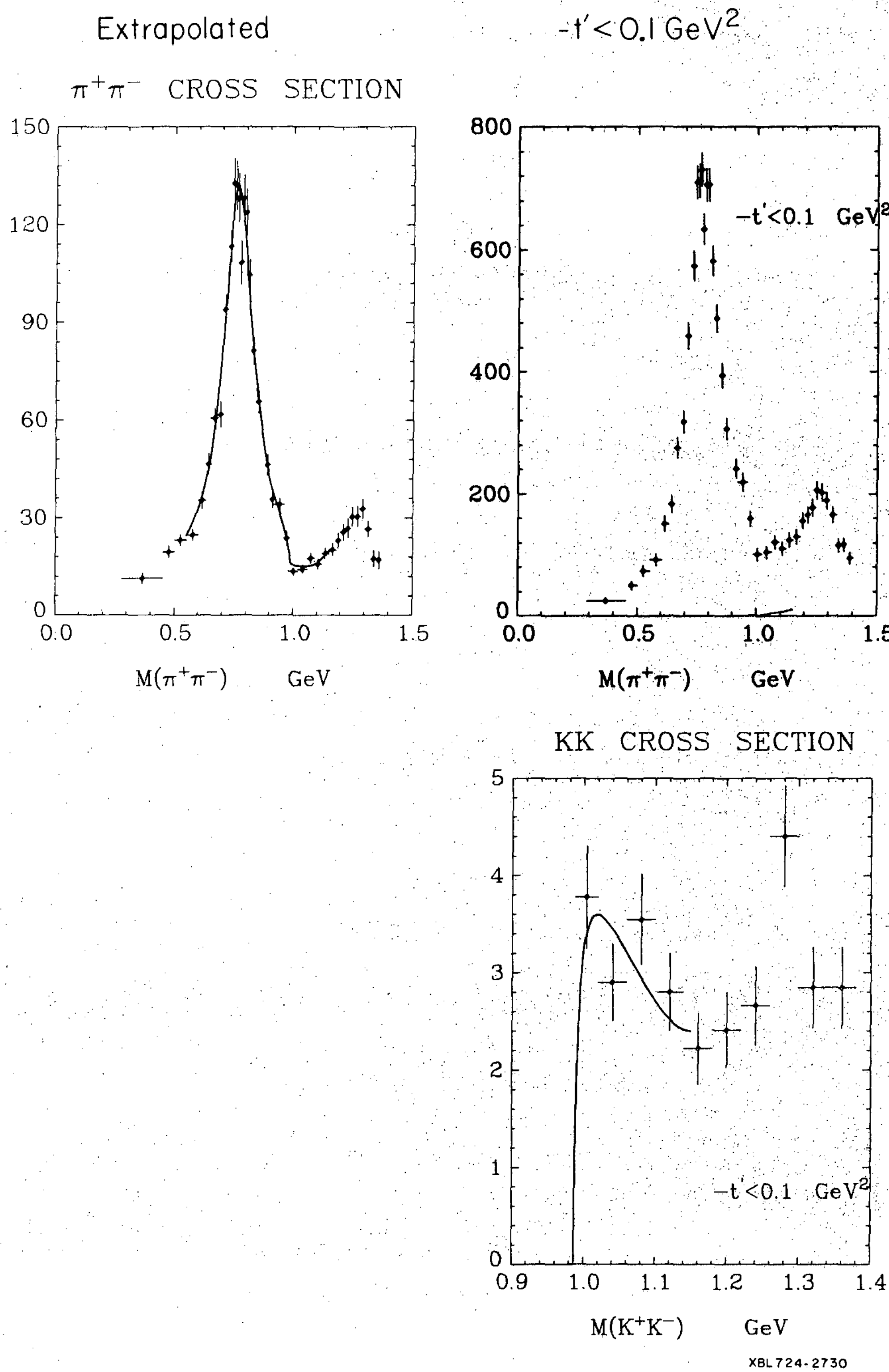

Fig. 2. Cross section (a) and $\langle Y_L^0 \rangle$ (b, c, d) for extrapolated data and $|t'_{p\Delta}| < 0.1$ GeV^2. The curves on the extrapolated data, and on the $K\bar{K}$ cross section for $|t'_{p\Delta}| < 0.1$ GeV^2 (a), are those corresponding to case-1 fit (see Table II).

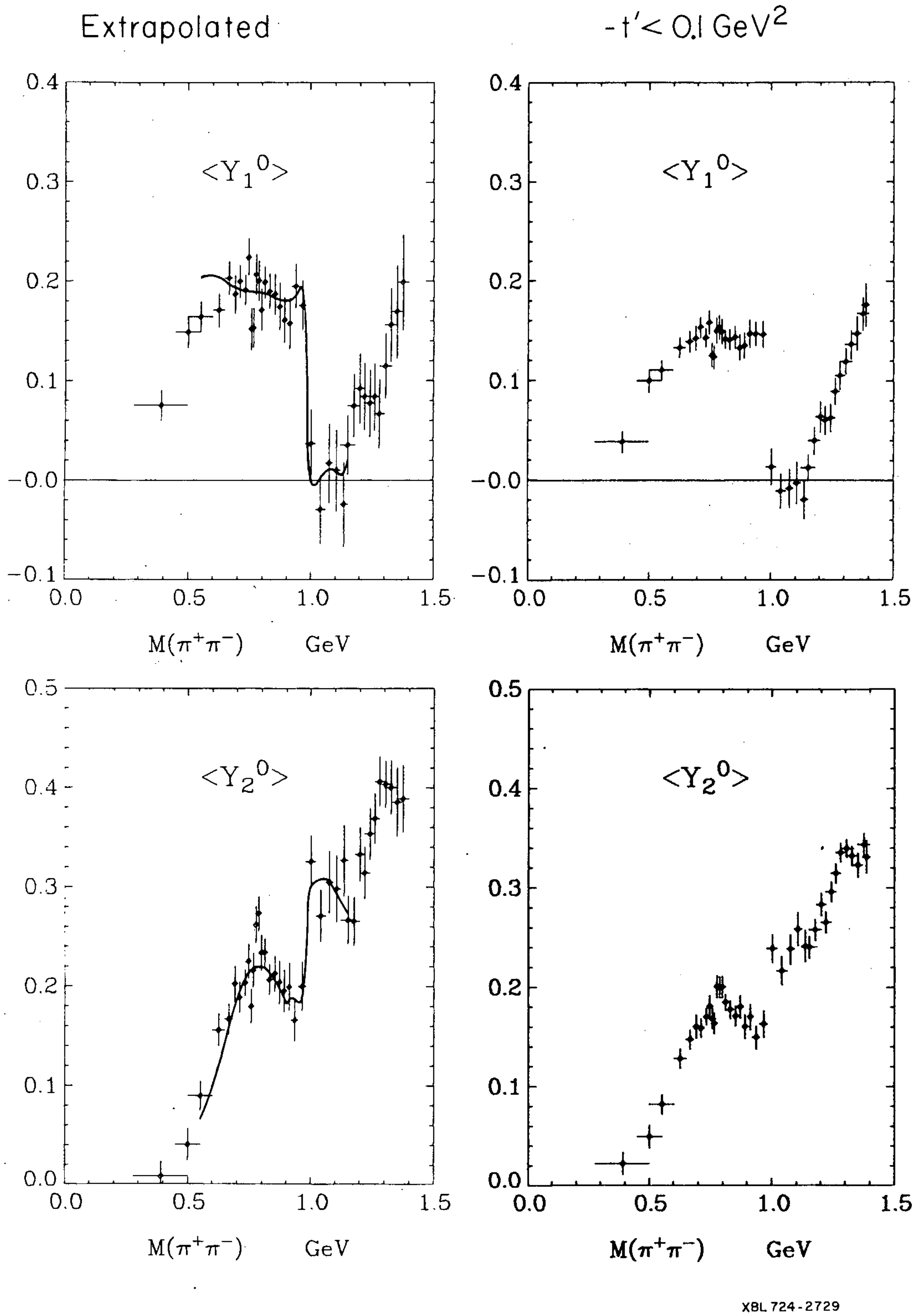
Extrapolated
-t'< 0.1 GeV^2
$<Y_1{}^0>$
$<Y_1{}^0>$
$<Y_2{}^0>$
$<Y_2{}^0>$
0.4
0.3
0.2
0.1
-0.0
-0.1
0.5
0.0
0.5
1.0
1.5
M($\pi^+\pi^-$) GeV
XBL 724-2729

Fig. 2b

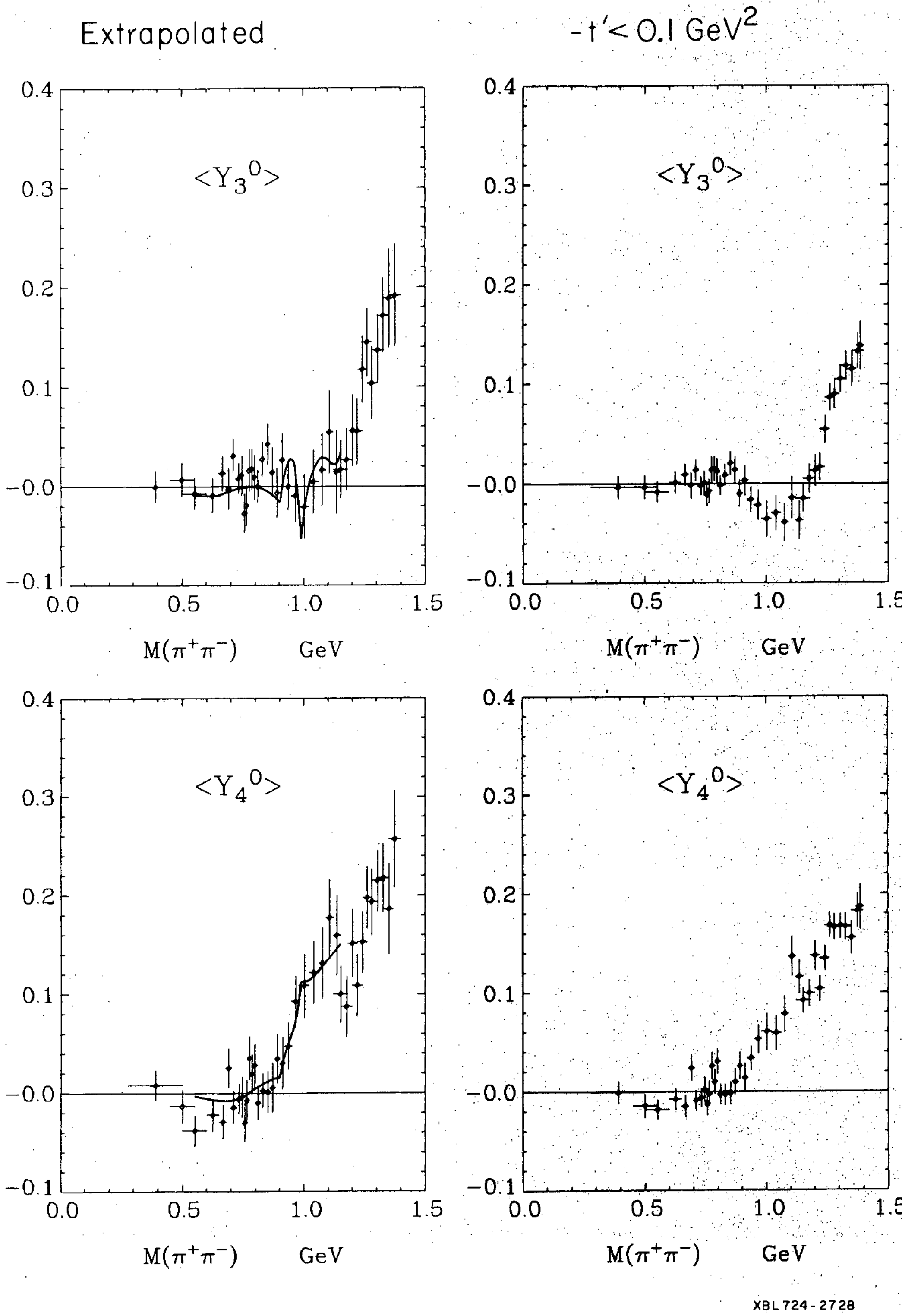
Extrapolated
-t'< 0.1 GeV²
<Y₃⁰>
<Y₄⁰>
0.4
0.3
0.2
0.1
-0.0
-0.1
0.0
0.5
1.0
1.5
M(π⁺π⁻) GeV
XBL 724-2728

Fig. 2c

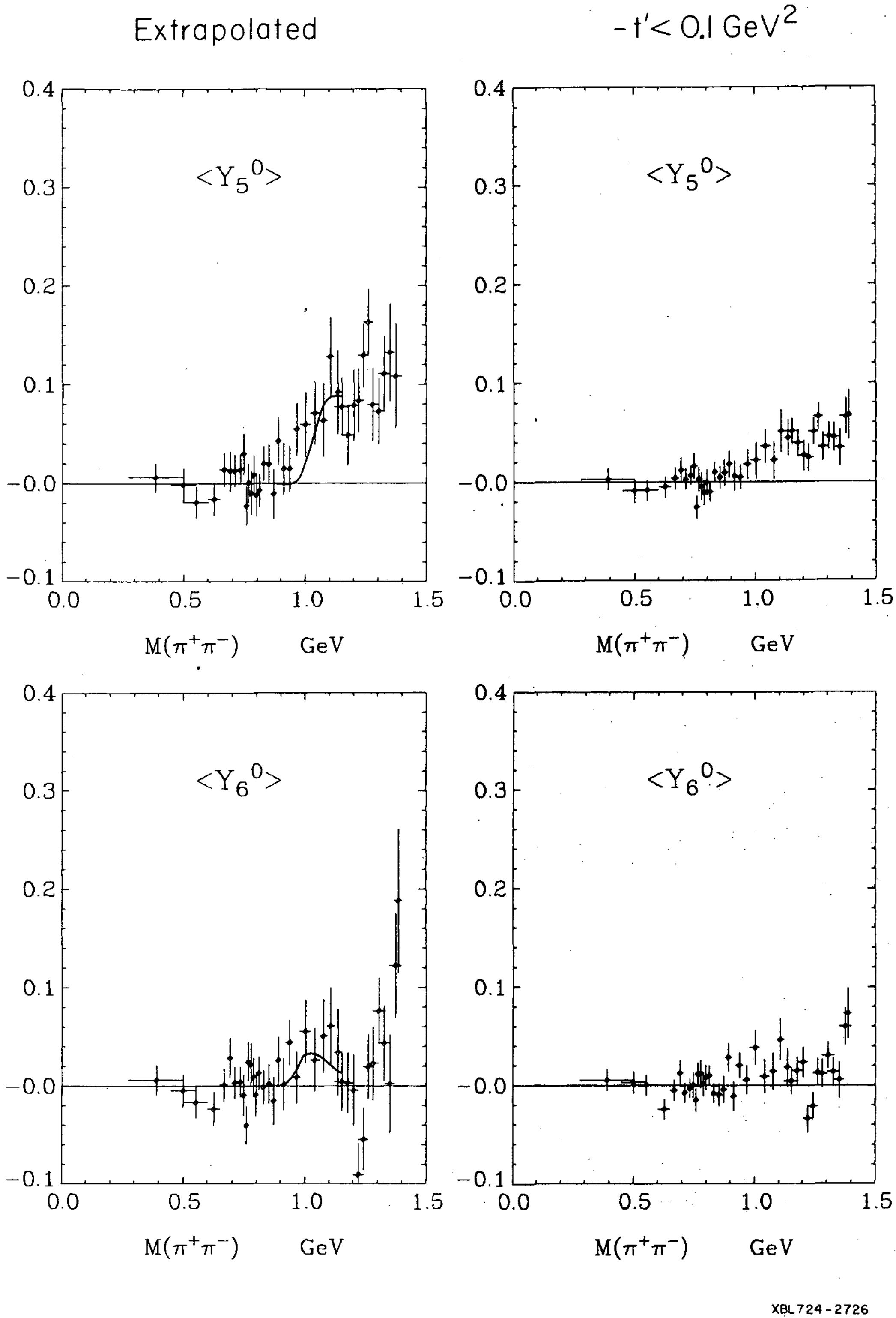

Extrapolated
-t'< 0.1 GeV^2
<Y_5^0>
<Y_5^0>
<Y_6^0>
<Y_6^0>
0.4
0.3
0.2
0.1
-0.0
-0.1
0.0
0.5
1.0
1.5
M($\pi^+\pi^-$) GeV
XBL 724-2726

Fig. 2d

U J J U U 8 U U J 4 3

provide useful guidelines as to where one can allow the various waves to become inelastic and put some constraints on the magnitude of the inelasticities. Note that the $\pi\pi$ s wave cannot contribute to the $\omega\pi$ channel so that the absence of events in the charged 4π channel suggests that a 2-channel ($\pi\pi$ and $K\bar{K}$) M-matrix may be an adequate representation for this wave.

III. EXTRAPOLATION TO π-POLE

If π exchange is dominant, the amplitude for the reaction $\pi^+ p \to \pi^+\pi^- \Delta^{++}$ is of the form (ignoring effects of absorption):

$$A(s,t) \propto \frac{\langle \pi^+ p \,|\, T \,|\, \pi^+ p \rangle \; \langle \pi^+\pi^- \,|\, T \,|\, \pi^+\pi^- \rangle}{t - \mu^2} + X, \tag{III.1}$$

where X stands for processes not produced by π exchange, e.g., A_2 exchange, $\pi^+ p \to A_2^+ p$, $\pi^+ p \to \pi^+ N^{*+}$, etc. When $t \to \mu^2$ the first term diverges while X remains finite. The hope then is that by extrapolating to $t = \mu^2$ one removes off-shell effects and non-π exchange contributions. After extrapolating the analysis becomes simpler in the sense that a standard phase shift analysis may be attempted. This simplicity is offset by the uncertainties in extrapolation procedures and the large increase in the statistical errors because of the need to divide the data in cells of t and $m_{\pi\pi}$. The uncertainty becomes larger the higher the mass because $|t_{min}|$ increases (at 1280 MeV, $t_{min} = -8\,\mu^2$).

A. Evaluation of the $\pi^+\pi^- \to \pi^+\pi^-$ Cross Section

In the case of one-pion exchange, the differential cross section for the process $\pi^+ p \to (\pi^+\pi^-)(\pi^+ p)$ is given by:

$$\frac{d^3\sigma}{dt\,dM\,dm} = \frac{1}{4\pi^3 P_I^2 E^2} (m^2 q_t \sigma_{\pi\pi}) \frac{G^2(t)}{(t-\mu^2)^2} (M^2 Q_t \sigma_{\pi p}), \tag{III.2}$$

where

P_I	= c.m. momentum,	m	= $\pi^+\pi^-$ invariant mass,
E	= c.m. energy,	M	= $\pi^+ p$ invariant mass,
$G(t)$	= form factor = 1 at π pole	$\sigma_{\pi\pi}$	= $\pi^+\pi^-$ cross section,
μ	= π mass,	$\sigma_{\pi p}$	= $\pi^+ p$ cross section,

q_t = virtual π momentum in $\pi^+\pi^-$ rest frame,

Q_t = incoming p momentum in $\pi^+ p$ rest frame.

In addition we define for later use:

q = outgoing π^+ momentum in $\pi^+\pi^-$ rest frame,

Q = outgoing p momentum in π^+p rest frame.

We have then:

$$q = \sqrt{\frac{m^2}{4} - \mu^2}\,, \qquad Q = \frac{1}{2M}\left\{[M^2-(m_p+\mu)^2][M^2-(m_p-\mu)^2]\right\}^{1/2},$$

$$q_t = \sqrt{\frac{(m^2+\mu^2-t)^2}{4m^2} - \mu^2}\,, \qquad Q_t = \sqrt{\frac{(M^2+m_p^2-t)^2}{4m^2} - m_p^2}\,.$$

The standard method of extrapolating is to calculate first:

$$\sigma_{OPE} \equiv \frac{1}{4\pi^3 P_I^2 E^2}\int_{m_1}^{m_2} dm \int_{t_1}^{t_2} dt \int_{M_1}^{M_2} dM\, m^2 q_t \frac{G^2(t)}{(t-\mu^2)^2}\, M^2 Q_t \sigma_{\pi p}. \qquad \text{(III.3)}$$

The above is the integral of Eq. (III.2), where we have set $\sigma_{\pi\pi} = 1$ mb and $\sigma_{\pi p}$ is the physical $\pi^+p \to \pi^+p$ scattering cross section. Then one fits to a polynomial in t the function

$$F(m,t) = \left(\int_{m_1}^{m_2} dm' \int_{t_1}^{t_2} dt' \int_{M_1}^{M_2} dM \frac{d^3\sigma}{dt'd\,Mdm'}\right) / \sigma_{OPE}\,, \qquad \text{(III.4)}^*$$

where $m = (m_1 + m_2)/2$ and $t = (t_1 + t_2)/2$. The cross section for $\pi^+\pi^-$ is then given by $\sigma_{\pi\pi}(m) = F(m, t = \mu^2)$.

With this procedure one usually needs high-order polynomials in t to obtain good results. A linear, or at most quadratic, extrapolation seems to be quite adequate for our data if we modify σ_{OPE} with Dürr-Pilkuhn form factors (DP). The disadvantage is that one must know in advance the amounts of each wave present. Fortunately the effect of DP form factors is not very drastic, so a rough estimate is quite adequate.

---

*The function F(m, t) is calculated taking the experimental cross section averaged over a bin in (t, m, M) and divided by σ_{OPE}.

The DP method consists in replacing:[5]

$$q_t \to q \qquad \text{for s-wave,}$$

$$q_t \to \left(\frac{q_t}{q}\right)^2 \left(\frac{1+R_p^2 q^2}{1+R_p^2 q_t^2}\right) q \qquad \text{for p wave} \qquad \text{(III.5)}$$

$$q_t \to \left(\frac{q_t}{q}\right)^4 \left(\frac{9+3\,R_d^2 q^2 + R_d^4 q^4}{9+3\,R_d^2 q_t^2 + R_d^4 q_t^4}\right) q \qquad \text{for d wave.}$$

For the Δ^{++} vertex the modification is slightly different:

$$Q_t \to \frac{(M+m_p)^2 - t}{(M+m_p)^2 - \mu^2} \left(\frac{Q_t}{Q}\right) \frac{1+R_\Delta^2 Q^2}{1+R_\Delta^2 Q_t^2}\, Q. \qquad \text{(III.6)}$$

Using these form factors, Wolf[6] could fit very well the t distributions in the ρ region (for $\pi^+ p \to \pi^+\pi^-\Delta^{++}$) at various beam energies with $R_p = 8.28 \pm 0.2$ GeV^{-1} and $R_\Delta = 3.97 \pm 0.11$ GeV^{-1}. In addition he had to introduce a slowly varying function:

$$G(t) = \frac{c-\mu^2}{c+t}, \qquad \text{where } c = 2.29 \pm 0.27\ (\text{GeV})^2.$$

These values have also given satisfactory fits to other reactions.[7] We made least-squares fits to t distributions for different $\pi\pi$ mass regions assuming that p wave and d wave are given by a ρ and f_0 mesons, and that the s wave is smooth and of the order of 13% of the cross section. We found that R_p and R_Δ are strongly correlated. If R_Δ is kept fixed at 4.0 GeV^{-1} then the best value for R_p was found to be 8.2 GeV^{-1}, in good agreement with Wolf's value. In Fig. 3 we show the result of a fit to the t distribution for $0.76 < M_{\pi\pi} < 0.78$ GeV. A least-squares fit to the f_0 region, keeping R_p and R_Δ fixed, showed that the value of R_d tends to be large and the fit is not very sensitive to it as long as $R_d \geqslant 14.0$ GeV^{-1}.

For calculating σ_{OPE} we used $R_\Delta = 4.0$ GeV^{-1}, $R_p = 8.2$ GeV^{-1}, $R_d = 14.0$ GeV^{-1} and took σ_{π^+p} from Carter et al.[8] We then did a least-squares fit to:

$$F(m,t) = a + bt \qquad (\text{Note that } \sigma_{\pi\pi} = a + b\mu^2) \qquad \text{(III.7)}$$

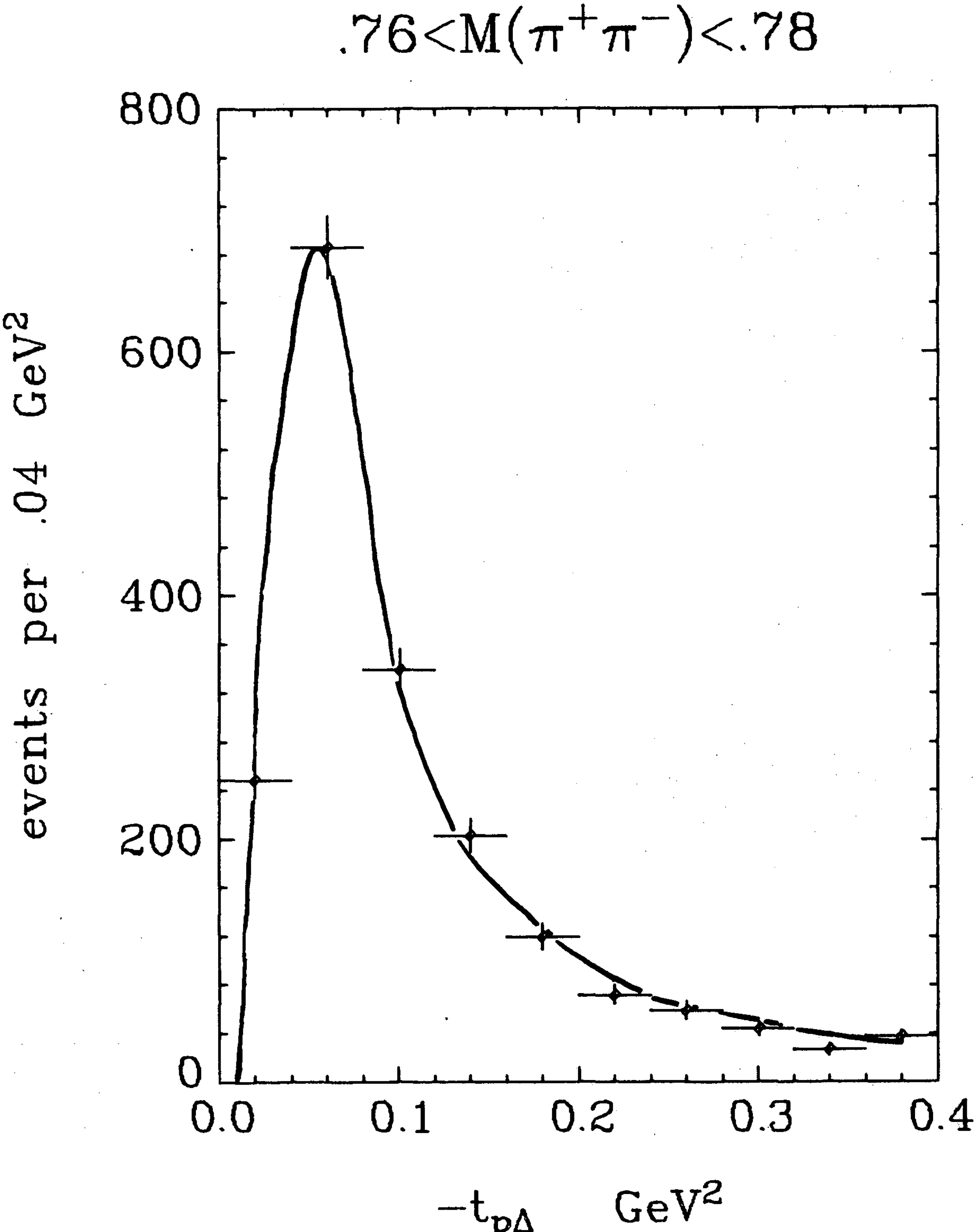

XBL724-2727

Fig. 3. $-t_{p\Delta}$ distribution for $0.76 < m_{\pi\pi} < 0.78$ GeV, for reaction $\pi^+p \rightarrow \pi^+\pi^-\Delta^{++}$. Curve corresponds to a fit with Dürr-Pilkuhn form factors.

to determine a and b for various mass bins. In the range 0.6 to 1.4 GeV the χ^2 for a linear fit was good, varying between 3.0 and 6.0 for five degrees of freedom. A quadratic fit did not improve χ^2 significantly in that energy range and the extrapolated values were compatible with the ones obtained by a linear extrapolation, but the errors on the extrapolated points were substantially larger. Below 600 MeV linear fits had poor χ^2 ($\geqslant 10.0$), while quadratic fits were found to be much better.

Extrapolations were tried for many different t intervals and also using the x variable of Baton et al.[9] Results varied little. The cross section shown in Fig. 2 was obtained with a linear extrapolation in t ($|t| < 0.4$ GeV^2) for points above 600 MeV. Below 600 MeV the extrapolation was quadratic in t. We obtained at 760-MeV $\sigma_{\pi\pi} = 133.4 \pm 4.8$ mb and at 1280-MeV $\sigma_{\pi\pi} = 31.2 \pm 2.0$ mb. The quoted errors are statistical. The unitary limit at those masses are:

I = 1	p wave	116 mb	at 760 MeV	$(12\,\pi\,\lambda\!\!\!^{-2})$
I = 0	s wave	17 mb	at 760 MeV	$(\frac{16}{9}\,\pi\,\lambda\!\!\!^{-2})$
I = 0	d wave	27.9 mb	at 1280 MeV	$(\frac{80}{9}\,\pi\,\lambda\!\!\!^{-2})$
I = 0	s wave	5.6 mb	at 1280 MeV	$(\frac{16}{9}\,\pi\,\lambda\!\!\!^{-2})$.

B. Extrapolation of Y_L^0 Moments

To extrapolate the moments we simply calculate:

$$\langle Y_L^0 \rangle \; (m,t) = \left(\sum_{i=1}^{N} Y^0_{L,i} \right) / N, \qquad \text{(III.8)}$$

where N = number of events in (m, t) cell, and fit $\langle Y_L^0 \rangle$ (m, t) for each m to a function a + bt. The $\pi\pi$ $\langle Y_L^0 \rangle$ is assumed to be equal to $\langle Y_L^0 \rangle$ (m, μ^2). Various intervals in t were tried, the results were always consistent with each other. The one shown on Fig. 2 is calculated for $|t| \leqslant 0.4$ GeV^2. Quadratic extrapolations only increased errors substantially without improving χ^2 significantly. Extrapolations using the variable x of Baton et al.[9] were found to be unsatisfactory, often giving values that were too high and would violate unitarity for some of the partial waves.

Since the moments are normalized we can neglect kinematic factors. In principle no factors would be needed if off-shell effects were the same for each partial wave. We find that by including DP form factors we can change the results by at most 1%, while the errors on extrapolated points are usually of the order of 10%. Unknown phases in the form factors may introduce larger corrections, but we

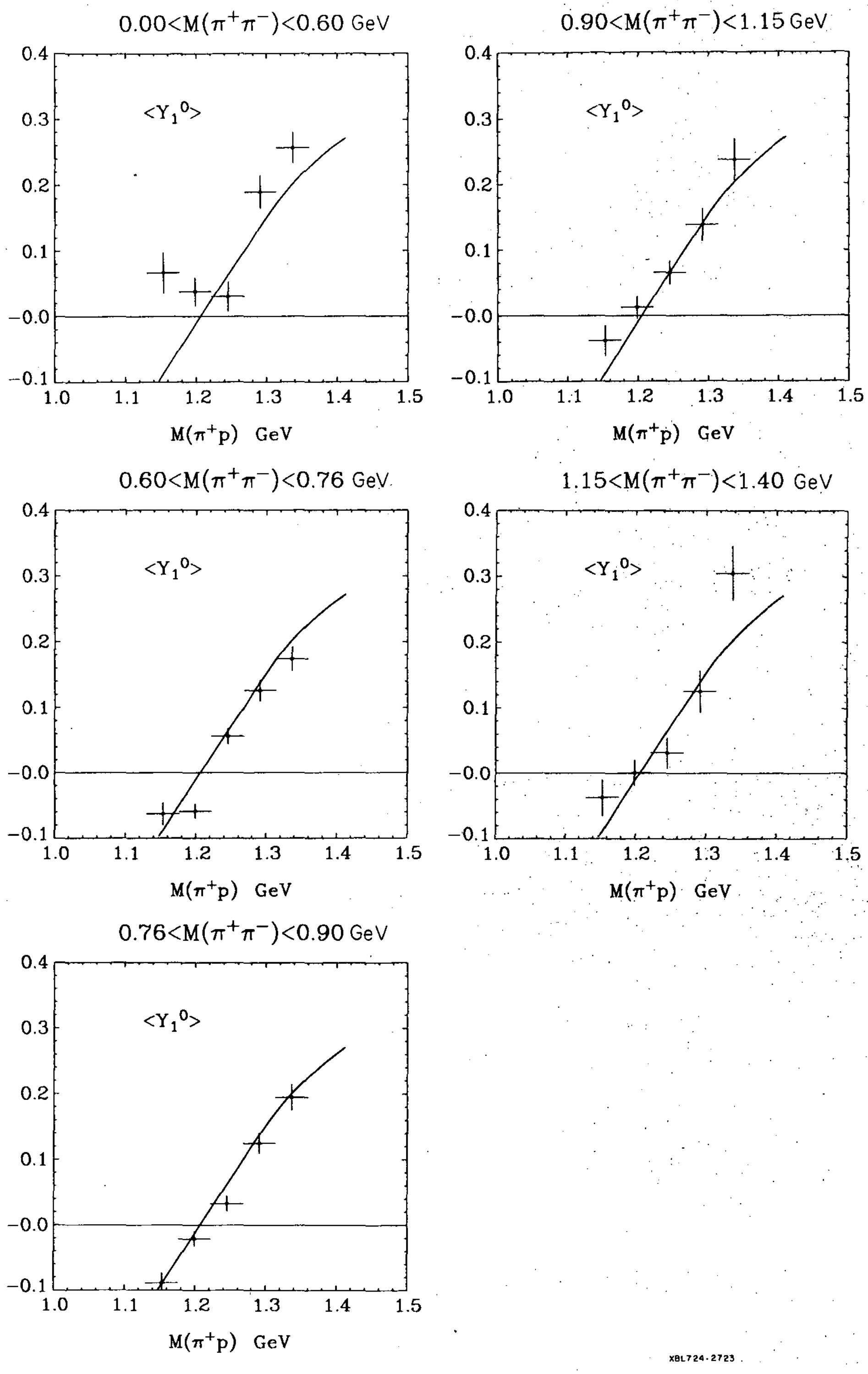

Fig. 4. Extrapolated $\langle Y_1^0 \rangle$ moments for π^+p vertex. Curves correspond to physical π^+p scattering.

know of no reliable way to estimate how important these phases may be.

The validity of the extrapolation procedure can be checked by looking at Y_ℓ^0 for the π^+p vertex as a function of π^+p and $\pi\pi$ mass. They should show no dependence on $\pi^+\pi^-$ mass. Linear extrapolations of Y_1^0 show striking agreement with the values for π^+p elastic scattering (Fig. 4), except for $\pi\pi$ mass below 600 MeV, which makes that region suspect. We have no adequate explanation as to why the extrapolation should fail at low $\pi\pi$ mass. It is worth emphasizing that if the Δ^{++} was produced by some other process than π exchange there is no reason to expect Y_1^0 to behave as observed in physical π^+p scattering, since that moment is determined by the interference between S and P waves; a pure Δ state would give $Y_1^0 = 0$.* These results give us more confidence in the validity of the extrapolation, but they do not constitute a proof.

IV. METHOD OF ANALYSIS

The partial wave amplitudes for $\pi^+\pi^-$ scattering may be written as:

$$S = \frac{2}{3}T_0^0 + \frac{1}{3}T_0^2, \qquad P = T_1^1,$$
$$D = \frac{2}{3}T_2^0 + \frac{1}{3}T_2^2, \qquad F = T_3^1. \tag{IV.1}$$

where

$$T_L^I = \frac{1}{2i}\left(\eta_L^I e^{2i\delta_L^I} - 1\right) \tag{IV.2}$$

Upper indices denote I - spin and lower indices angular momentum L. The cross section and the Y_L^0 moments are, in term of the above amplitudes:

*The extrapolated Y_2^0 moment also agrees quite well with the one observed in physical π^+p scattering; but this is a much weaker check since any reaction where the P_{33}, m = 3/2, wave dominates will give a similar Y_2^0 moment.

$$\sigma_{\pi\pi} = 4\pi \lambda\!\!\!^{-2} \left(|S|^2 + 3|P|^2 + 5|D|^2 + 7|F|^2 \right),$$

$$\langle Y_1^0 \rangle = \left(\sqrt{\frac{3}{\pi}}\, \mathrm{Re}(S^*P) + 2\sqrt{\frac{3}{\pi}}\, \mathrm{Re}(P^*D) + 3\sqrt{\frac{3}{\pi}}\, \mathrm{Re}(D^*F) \right) \frac{4\pi \lambda\!\!\!^{-2}}{\sigma_{\pi\pi}},$$

$$\langle Y_2^0 \rangle = \left[\frac{3}{\sqrt{5\pi}} |P|^2 + \sqrt{\frac{5}{\pi}}\, \mathrm{Re}(S^*D) + \frac{5}{7}\sqrt{\frac{5}{\pi}}\, |D|^2 + \frac{9}{\sqrt{5\pi}}\, \mathrm{Re}(P^*F) \right.$$

$$\left. + \frac{14}{3\sqrt{5\pi}} |F|^2 \right] \frac{4\pi \lambda\!\!\!^{-2}}{\sigma_{\pi\pi}}, \qquad \text{(IV.3)}$$

$$\langle Y_3^0 \rangle = \left[\frac{9}{\sqrt{7\pi}}\, \mathrm{Re}(P^*D) + \frac{4}{3}\sqrt{\frac{7}{\pi}}\, \mathrm{Re}(D^*F) + \sqrt{\frac{7}{\pi}}\, \mathrm{Re}(S^*F) \right] \frac{4\pi \lambda\!\!\!^{-2}}{\sigma_{\pi\pi}},$$

$$\langle Y_4^0 \rangle = \left[\frac{15}{7\sqrt{\pi}} |D|^2 + \frac{4}{\sqrt{\pi}}\, \mathrm{Re}(P^*F) + \frac{21}{11\sqrt{\pi}} |F|^2 \right] \frac{4\pi \lambda\!\!\!^{-2}}{\sigma_{\pi\pi}},$$

$$\langle Y_5^0 \rangle = \frac{50}{3\sqrt{11\pi}}\, \mathrm{Re}(D^*F)\, \frac{4\pi \lambda\!\!\!^{-2}}{\sigma_{\pi\pi}},$$

$$\langle Y_6^0 \rangle = \frac{350}{33\sqrt{13\pi}} |F|^2\, \frac{4\pi \lambda\!\!\!^{-2}}{\sigma_{\pi\pi}}.$$

The total number of parameters to be determined at each value of $m_{\pi\pi}$ is 12, assuming partial waves up to $L = 3$ are important. It is not possible to determine them by an energy independent-analysis using the reaction $\pi^+ p \rightarrow \pi^+ \pi^- \Delta^{++}$ alone,* since we only have seven constraints—six moments and the cross section. In order to extract phases and inelasticities we parametrize them as functions of $\pi\pi$ mass (or momentum) and then do a least-squares fit to the moments and the cross section.

---

*Even with an energy-dependent analysis, one cannot determine all 12, one needs data from other charged states to be able to separate $I = 2$ and $I = 0$ components.

0 0 0 0 3 8 0 0 2 4 0

The parametrization we use is the following:

A. <u>p Wave, f Wave, and I = 0 d Wave</u>

For the I = 1 p wave and f wave, and the I = 0 d wave,

$$T_L^{\ I} = \frac{\eta_B^{(\ell)}\, e^{2i\delta_B^{(\ell)}} - 1}{2i} + e^{2i\phi^{(\ell)}}\, BW^{(\ell)}, \qquad \text{(IV.4)}$$

where

$$\eta_B^{(\ell)} = \begin{cases} 1 & \text{below } \omega\pi \text{ threshold} \\ e^{-\nu} & \text{above } \omega\pi \text{ threshold,} \end{cases}$$

$$\nu = \left(q - q_{th}\right)^{2\ell+1} \left(\sum_{n=o}^{1} b_n^{(\ell)} q^n\right)^2 , \qquad \text{(IV.5)}$$

$$\delta_B^{(\ell)} = q^{2\ell+1} \sum_{n=o}^{N} \left(a_n^{(\ell)} q^n\right) , \qquad \text{(IV.6)}$$

q = $\pi\pi$ c.m. momentum,

q_{th} = q evaluated at $\omega\pi$ threshold,

$$BW^{(\ell)} = \frac{\Gamma_{\pi\pi}^{(\ell)}/2}{E_R^{(\ell)} - E - (i\Gamma^{(\ell)}/2)} , \qquad \text{(IV.7)}$$

$$\Gamma_{\pi\pi}^{(\ell)} = \Gamma_R^{(\ell)} \left(\frac{q}{q_R^{(\ell)}}\right)^{2\ell+1} \frac{2E_R^{(\ell)}}{E_R^{(\ell)} + E} \frac{D_\ell^R}{D_\ell} , \qquad \text{(IV.8)}$$

E = $\pi\pi$ c.m. energy,

$q_R^{(\ell)}$ = q evaluated at $E = E_R$,

D_ℓ^R = D_ℓ evaluated at $E = E_R$.

a) For the p wave,

$$\Gamma^{(1)} = \Gamma_{\pi\pi}^{(1)} + \Gamma_{\omega\pi}$$

$$D_1 = \frac{q^2 r_\rho^2}{1 + q^2 r_\rho^2} \tag{IV.9}$$

$$\Gamma_{\omega\pi} = \begin{cases} 0 \text{ below } \omega\pi \text{ threshold} \\ g^2_{\omega\rho\pi}\ q^3_{\omega\pi} \text{ above } \omega\pi \text{ threshold.} \end{cases}$$

There are eight parameters describing this wave which must be obtained from the fit, namely $a_0^{(1)}$, $a_1^{(1)}$, $b_0^{(1)}$, $b_1^{(1)}$, $\Gamma_R^{(1)}$, $E_R^{(1)}$ $g_{\rho\omega\pi}$, and r_ρ. It turns out that $g_{\rho\omega\pi}$ is strongly correlated with $b_0^{(1)}$ and $b_1^{(1)}$, so $g^2_{\rho\omega\pi}$ was fixed* at 0.6 GeV^{-2} and only seven parameters allowed to vary.

b) For the d wave,

$$\Gamma^{(2)} = \Gamma_{\pi\pi}^{(2)} + \Gamma_{KK} ,$$

$$D_2 = \frac{q^4 r_f^4}{g + 3q^2 r_f^2 + q^4 R_f^4} , \tag{IV.10}$$

$$\Gamma_{KK} = \begin{cases} 0 \text{ below } K\bar{K} \text{ threshold} \\ g_{KK} \left(\dfrac{q_{KK}}{q^R_{KK}} \right)^5 \text{ above } K\bar{K} \text{ threshold,} \end{cases}$$

$$q_{KK} = \text{c.m. momentum of } K\bar{K} \text{ system,}$$

$$q^R_{KK} = q_{KK} \text{ at } E = E_R^2 .$$

---

*To compute this number we used the $\rho\omega\pi$ coupling constant calculated by Gell-Mann, Sharp, and Wagner[10]; the fits are rather insensitive to the value of $g_{\rho\omega\pi}$.

0 0 0 0 3 8 0 0 2 4 7

In this case, since the overall fit is only up to 1.15 GeV, $\Gamma_R^{(2)}$, $E_R^{(2)}$, and r_f are kept fixed at values obtained from a fit to the mass distribution alone ($\Gamma_R^{(2)} = 0.18$ GeV, $E_R^{(2)} = 1.28$ GeV, $r_f = 3.0$ GeV^{-1}), and $g^2_{K\bar{K}}$ is set at 0.04. This value was chosen by comparing the number of events in the $K\bar{K}$ channel to the number of events in the $\pi^+\pi^-$ channel in the f_0 region for $|t'| < 01\,\mathrm{GeV}^2$. At such low t the A_2 contribution to $K\bar{K}$ in that mass region should be quite small. The fits are not particularly sensitive to the value of g^2_{KK} as long as $g^2_{KK} < 0.1$. The parameters left free are five: $a_0^{(2)}$, $a_1^{(2)}$, $a_2^{(2)}$, $b_0^{(2)}$, and $b_1^{(2)}$.*

The parametrization for the p wave, f wave, and I = 0 d wave has the expected threshold behavior for δ and is a reasonable approximation for η. In addition it is a good approximation to the expected behavior of an inelastic resonance plus inelastic background in the elastic channel if the pole is not close to a threshold.[11] For certain values of $\phi^{(\ell)}$ the parametrization may violate unitarity at some energies. We found that setting $\phi^{(\ell)} = \delta_B^{(\ell)}$ unitarity was never violated in the fitted region. We emphasize that we are not attempting to separate the amplitude into background plus a resonance, we are simply using what we consider a reasonable approximation to the dependence of δ and η on the energy in order to extract them from the data. No particular significance should be attached to the values obtained for the parameters themselves.

B. I = 2 s and d waves

The fits are not very sensitive to the I = 2 amplitudes which are known to be fairly small in the fitted region. We set $\eta_0^2 = \eta_2^2 = 1$ throughout. For the I = 2 s wave we take:

$$\delta_0^2 = q \sum_{n=0}^{5} C_n q^{2n}$$

where the various coefficients were obtained by fitting known data.[12]

The δ_2^2 phase is poorly known at present but is believed to be negative.[13] For the I = 2 d wave we set

$$\delta_2^2 = a\, q^5,$$

where $a = -100\ \mathrm{GeV}^{-5}$. This reproduces reasonably well the values given by Baton et al.[9]

*The I = 0 d-wave cannot couple to $\omega\pi$ channel, nevertheless we allowed the background to become inelastic around 900 MeV. Results change very little if we don't allow it to become inelastic before 980 MeV.

C. I = 0 s wave

The I = 0 s-wave amplitude is parametrized in terms of a 2×2 M-matrix;[14] we assume that only the $\pi\pi$ and $K\bar{K}$ channels are important. As noted earlier data from other channels indicate that this is a reasonable assumption.[3]

Set
$$T_0^0 = \begin{pmatrix} T_{11} & T_{12} \\ T_{12} & T_{22} \end{pmatrix},$$

where
$$T_{11} = \pi^+\pi^- \to \pi^+\pi^- \quad \text{s-wave amplitude},$$
$$T_{12} = \pi^+\pi^- \to K\bar{K} \quad \text{s-wave amplitude},$$
$$T_{22} = K\bar{K} \to K\bar{K} \quad \text{s-wave amplitude}.$$

These amplitudes are normalized so that

$$\sigma_{ij} = 4\pi\lambda\!\!\!^{-2} \,|T_{ij}|^2.$$

In terms of the M-matrix,

$$T = k^{1/2}(M - ik)^{-1} k^{1/2},$$

$$k = \text{diagonal matrix of momenta.}$$

Explicitly, T is given by

$$T = \frac{1}{D}\begin{bmatrix} k_1(M_{22} - ik_2) & -\sqrt{k_1k_2}\,M_{12} \\ -\sqrt{k_1k_2}\,M_{12} & k_2(M_{11} - ik_1) \end{bmatrix}, \qquad \text{(IV.11)}$$

where

$$D = (M_{11} - ik_1)(M_{22} - ik_2) - M_{12}^2,$$

$k_1 = \pi$ momentum in $\pi\pi$ c.m. system,

$k_2 = K$ momentum in $K\bar{K}$ c.m. system.

0 0 0 0 3 8 0 0 2 4 8

Table I. Parametrization of partial waves.

Partial wave	Parametrization	Number of free parameters
I=0 s wave	2×2 M-matrix coupling $\pi\pi$ and $K\bar{K}$ channels	7
I=1 p wave[a]	ρ resonance + background, both become inelastic at 900 MeV	7
I=0 d wave[a]	f_0 resonance coupled to $\pi\pi$ and $K\bar{K}$ + background which becomes inelastic at 900 MeV	5
I=1 f wave[a]	Elastic g resonance + background which becomes inelastic at 900 MeV	5
I=2 s wave	$\eta_2^0=1,\ \delta_2^0= q \sum_{n=0}^{5} c_n q^{2n}$	0
I=2 d wave	$\eta_2^2=1,\ \delta_2^2 = aq^5$	0

[a]Parametrization for this wave is similar to one used by Roper, Wright, and Feld to calculate πN phase shifts.[11]

This representation—provided M is real and symmetric—with the prescription $k_2 \to i\,|k_2|$ below $K\bar{K}$ threshold satisfies the requirements of analyticity and unitarity under the assumption that we can neglect channels other than $\pi\pi$ and $K\bar{K}$. The M-matrix elements are taken of the form

$$M_{ij} = M^0_{ij} + M^1_{ij}\,(s-s_0), \tag{IV.12}$$

where $s = m^2_{\pi\pi}$ and $s_0 = s$ at $K\bar{K}$ threshold. It is evident that the results are independent of the choice of s_0. A reasonable fit can be obtained with a linear expansion of M^0_{ij}, but χ^2 improves substantially if one more term is added to either M_{12} or M_{22}. Adding more terms only increases the correlations between parameters without changing χ^2 significantly. So we use a linear expansion in M_{11} and M_{22} and a quadratic one in M_{12}. This gives seven free parameters for the I = 0 s-wave amplitude. From the data in the physical region (for which we have ±8-MeV resolution, FWHM), we can infer that the s-wave amplitude should be almost zero within 10 MeV of $K\bar{K}$ threshold, and one could force that constraint on the fit setting $M^0_{22} = 0$.

V. SOLUTIONS

We have 24 parameters to be determined from the data. The parametrization is summarized in Table I. We fit the extrapolated moments up to Y^0_6 and the cross sections ($\pi^+\pi^- \to \pi^+\pi^-$, $\pi^+\pi^- \to K\bar{K}$) between 550 and 1150 MeV with a total of 171 points.* We did a large number of fits starting from different initial values and varying slightly the parametrization for each of the waves. We must emphasize that our parametrization is by no means unique and other parametrizations might serve equally well. The χ^2 for the best fits range from 150 to 160, which for 147 degrees of freedom corresponds to confidence levels between 40% and 20%. In Table II we list some properties of the two fits with similar χ^2 which differed the most. The curves shown on Fig. 2 are for case 1; the parameters and error matrix for this case are given in Tables III and IV.

Overall the fit seems reasonably good but there are some noticeable discrepancies. Between 550 and 650 MeV, predicted Y^0_1 is systematically high, Y^0_2 systematically low, and Y^0_4 is not as negative as the data. It might be possible to improve the fit if the f wave is more negative in that region than the present parametrization permits. In the region 760 to 800 MeV the $\pi\pi$ cross section

*We used the computer program OPTIME[15] for minimizing χ^2.

Table II. Properties of two different fits.

Case	Description	Degrees of freedom	χ^2	S^* pole	ϵ pole
1	Background phase for $\ell \neq 0$ waves given by: $\delta_B^{(\ell)} = q^{2\ell+1} \sum_{n=0}^{N} a_n^{(\ell)} q^n$ M-matrix elements: $M_{ij} = M_{ij}^0 + M_{ij}^1 (s-s_0) + M_{ij}^2 (s-s_0)^2$ See text for complete description	147	152.2	980 ± 6 $-i(37 \pm 8)$ II sheet	600 ± 100 $-i(250 \pm 70)$ II sheet
2	Background phase for $\ell \neq 0$ waves given by: $\delta_B^{(\ell)} = q\, D_\ell(q) \sum_{n=0}^{N} a_n^{(\ell)} q^n$ M-matrix elements: $M_{ij} = M_{ij}^0 + M_{ij}^1 (E-E_0) + M_{ij}^2 (E-E_0)^3$ Otherwise same as case 1.	147	153.6	975 ± 6 $-i(39 \pm 8)$ II sheet	650 ± 70 $-(150 \pm 50)$ IV sheet

Table III. Parameters obtained from fit (case 1).[a]

I=0 s wave	$M^0_{11} = -3.3 \pm 2.2$	$M^1_{11} = -0.45 \pm 0.33$		
	$M^0_{12} = 2.66 \pm 0.42$	$M^1_{12} = -0.569 \pm 0.24$	$M^2_{12} = 0.003 \pm 0.002$	
	$M^0_{22} = 0.034 \pm 0.06$	$M^1_{22} = -0.475 \pm 0.25$		
I=1 p wave	$E_R^{(1)} = 0.78 \pm 0.004$ GeV	$\Gamma_R^{(1)} = 0.17 \pm 0.01$ GeV	$r_\rho = 1.1 \pm 0.9\ \mathrm{GeV}^{-1}$	
	$a_0^{(1)} = 0.48 \pm 0.25$	$a_1^{(1)} = -0.022 \pm 0.064$		
	$b_0^{(1)} = -0.142 \pm 3.0$	$b_1^{(1)} = -0.215 \pm 0.7$		
I=0 d wave	$a_0^{(2)} = -0.14 \pm 0.09$	$a_1^{(2)} = 0.078 \pm 0.05$	$a_2^{(2)} = -0.010 \pm 0.008$	
	$b_0^{(2)} = 18.1 \pm 4.8$	$b_1^{(2)} = -4.5 \pm 1.2$		
I=1 f wave	$a_0^{(3)} = -0.011 \pm 0.006$	$a_2^{(3)} = 0.0057 \pm 0.003$	$a_3^{(3)} = -0.0007 \pm 0.0004$	
	$b_0^{(3)} = 2.45 \pm 0.27$	$b_1^{(2)} = -5.53 \pm 1.83$		
I=2 d wave		$a = -100\ \mathrm{GeV}^{-5}$ (fixed)		
I=2 s wave	$c_0 = -2.2 \times 10^{-2}$	$c_1 = -4.17 \pm 10^{-2}$	$c_2 = 1.48 \times 10^{-2}$	$c_3 = -2.49 \times 10^{-3}$
	$c_4 = 1.76 \times 10^{-4}$	$c_5 = -4.24 \times 10^{-6}$		
		(fixed)		

[a] Correlations between parameters are large; for any computation using these parameters the full error matrix should be used (Table IV). Unless otherwise indicated, units are in appropriate powers of μ (π-mass).

Table IV. Normalized error matrix $\left(E_{ij} = \dfrac{\langle \delta x_i \delta x_j \rangle}{\sqrt{\langle \delta x_i^{\,2} \rangle \langle \delta x_j^{\,2} \rangle}}\right)$

	M^0_{11}	M^0_{12}	M^1_{11}	M^1_{12}	M^1_{22}	M^2_{12}	M^0_{22}	$a_0^{(1)}$	$a_1^{(1)}$	$E_R^{(1)}$	$\Gamma_R^{(1)}$	r_ρ	$a_0^{(2)}$	$a_1^{(2)}$	$a_2^{(2)}$	$a_0^{(3)}$	$a_1^{(3)}$	$b_0^{(1)}$	$b_1^{(1)}$	$b_0^{(2)}$	$b_1^{(2)}$	$a_2^{(3)}$	$b_0^{(3)}$	$b_1^{(3)}$
M^0_{11}	1.00	-.85	1.00	-.99	.95	.93	-.19	.06	-.04	.06	.16	-.05	-.14	.13	-.12	-.04	.03	-.04	.05	-.02	.10	-.09	.07	-.15
M^0_{12}	-.85	1.00	-.84	.87	-.91	-.81	-.06	-.08	.07	-.05	-.08	.03	.16	-.17	.17	-.02	.04	-.02	.02	-.05	-.04	.04	.04	-.00
M^1_{11}	1.00	-.84	1.00	-1.00	.95	.92	-.17	.07	-.04	.06	.16	-.05	-.14	.14	-.12	-.05	.03	-.03	.05	-.02	.10	-.10	.07	-.15
M^1_{12}	-.99	.87	-1.00	1.00	-.97	-.92	.17	-.07	.05	-.05	-.15	.04	.15	-.15	.14	.04	-.03	.02	-.03	.01	-.09	.09	-.06	.13
M^1_{22}	.95	-.91	.95	-.97	1.00	.89	-.17	.07	-.06	.04	.11	-.01	-.17	.17	-.17	-.02	.01	.01	-.01	-.01	.06	-.05	.01	-.06
M^2_{12}	.93	-.81	.92	-.92	.89	1.00	-.28	.05	-.04	.02	.05	-.02	-.09	.09	-.09	-.05	.04	-.01	.02	-.03	.08	-.08	.04	-.11
M^0_{22}	-.19	-.06	-.17	.17	-.17	-.28	1.00	.08	-.08	.03	-.03	-.07	-.07	.09	-.11	.03	-.04	.05	-.05	.05	.07	-.07	-.02	.06
$a_0^{(1)}$	.06	-.08	.07	-.07	.07	.05	.08	1.00	-.98	.75	.11	-.66	-.26	.25	-.24	.13	-.15	.33	-.24	.16	.27	-.26	-.30	.28
$a_1^{(1)}$	-.04	.07	-.04	.05	-.06	-.04	-.08	-.98	1.00	-.64	.06	.52	.27	-.27	.27	-.11	.13	-.39	.31	-.14	-.20	.19	.28	-.25
$E_R^{(1)}$	.06	-.05	.06	-.05	.04	.02	.03	.75	-.64	1.00	.58	-.56	-.19	.17	-.15	.12	-.14	.03	.03	.14	.28	-.28	-.19	.19
$\Gamma_R^{(1)}$	.16	-.08	.16	-.15	.11	.05	-.03	.11	.06	.58	1.00	-.34	-.15	.11	-.07	.06	-.07	-.19	.20	.07	.28	-.28	-.09	.10
r_ρ	-.05	.03	-.05	.04	-.01	-.02	-.07	-.66	.52	-.56	-.34	1.00	-.01	.02	-.04	-.17	.19	-.20	.11	-.20	-.44	.43	.41	-.39
$a_0^{(2)}$	-.14	.16	-.14	.15	-.17	-.09	-.07	-.26	.27	-.19	-.15	-.01	1.00	-.99	.98	-.16	.16	-.33	.33	-.17	-.19	.19	.10	-.14
$a_1^{(2)}$	.13	-.17	.14	-.15	.17	.09	.09	.25	-.27	.17	.11	.02	-.99	1.00	-.99	.15	-.16	.37	-.37	.16	.19	-.19	-.11	.17
$a_2^{(2)}$	-.12	.17	-.12	.14	-.17	-.09	-.11	-.24	.27	-.15	-.07	-.04	.98	-.99	1.00	-.14	.15	-.40	.41	-.16	-.18	.19	.13	-.20
$a_0^{(3)}$	-.04	-.02	-.05	.04	-.02	-.05	.03	.13	-.11	.12	.06	-.17	-.16	.15	-.14	1.00	-1.00	.12	-.11	.99	.08	-.07	-.15	.13
$a_1^{(3)}$	.03	.04	.03	-.03	.01	.04	-.04	-.15	.13	-.14	-.07	.19	.16	-.16	.15	-1.00	1.00	-.13	.11	-1.00	-.09	.08	.19	-.16
$b_0^{(1)}$	-.04	-.02	-.03	.02	.01	-.01	.05	.33	-.39	.03	-.19	-.20	-.33	.37	-.40	.12	-.13	1.00	-.99	.13	.07	-.07	-.17	.29
$b_1^{(1)}$	.05	.02	.05	-.03	-.01	.02	-.05	-.24	.31	.03	.20	.11	.33	-.37	.41	-.11	.11	-.99	1.00	-.12	-.03	.03	.14	-.28
$b_0^{(2)}$	-.0	-.05	-.02	.01	.01	-.03	.05	.16	-.14	.14	.07	-.20	-.17	.16	-.16	.99	-1.00	.13	-.12	1.00	.10	-.09	-.21	.18
$b_1^{(2)}$	.10	-.04	.10	-.09	.06	.08	.07	.27	-.20	.28	.28	-.44	-.19	.19	-.18	.09	-.09	.07	-.03	.10	1.00	-1.00	-.27	.12
$a_2^{(3)}$	-.09	.04	-.10	.09	-.05	-.08	-.07	-.26	.19	-.28	-.28	.43	.19	-.19	.19	-.07	.08	-.07	.03	-.09	-1.00	1.00	.26	-.11
$b_0^{(3)}$	.07	.04	.07	-.06	.01	.04	-.02	-.30	.28	-.19	-.09	.41	.10	-.11	.13	-.15	.19	-.17	.14	-.21	-.27	.26	1.00	-.90
$b_1^{(3)}$	-.15	-.00	-.15	.13	-.06	-.11	.06	.28	-.25	.19	.10	-.39	-.14	.17	-.20	.13	-.16	.29	-.28	.18	.12	-.11	-.90	1.00

and Y_1^0 have a dip and Y_2^0 a spike not predicted by the fit. If we believe that in that region only s and p waves are important, then the value for extrapolated Y_2^0 is unphysical. The contribution to χ^2 of that region is 40 (for 9 points) so it was excluded from the final fits. Since this effect occurs very close to the ω mass (783 MeV), it is certainly possible that it is associated with ρ-ω interference. If this is the case it is somewhat surprising that we observe the effect on the extrapolated data, since the ω cannot be produced by π exchange (at least not strongly); thus, it is part of the background that should disappear when we extrapolate. On the contrary, the extrapolation enhances the effect. A similar phenomenon was observed in the extrapolation of ππ cross section by Colton et al.[16] for the reaction $\pi^+ p \rightarrow \pi^+\pi^-\Delta^{++}$ at 8 GeV/c. To see if this enhancement was due simply to the conditions of the extrapolation [i.e., linear and including events up to $|t_{p\Delta}| = 0.4\,(\text{GeV/c})^2$] we performed quadratic and linear extrapolations using different cutoffs for t in that region. The quadratic extrapolations tend to enhance the effect even more; choosing smaller cutoffs only increased errors without changing results significantly. An explanation for this effect, which is consistent with data for reaction $\pi^+ p \rightarrow \omega\Delta^{++}$ at 7.1 GeV/c, is that at small t the ω is produced mainly by B exchange with zero helicity. In this case ρ-ω interference is most pronounced at small t, distorting results of extrapolation to the π pole.

In order to fit the moments Y_3^0 to Y_6^0 above 900 MeV, we needed all waves (excluding $\ell = 0$ and $I = 2$ amplitudes) to become inelastic at the ωπ threshold.* If the ω had zero width this threshold would be at 920 MeV; the fits improved somewhat if we allowed the threshold to start at 900 MeV instead. We also found that we could not fit very well the moments Y_4^0 to Y_6^0 with the parametrization for $\eta_3{}^1$ described earlier [Eq. IV.5)]. In addition, by 1.0 GeV, $\eta_3{}^1$ was too small to be consistent with data in other channels (predicting an order-of-magnitude more events than observed). A better fit is obtained if we take instead:

$$\eta_B^{(3)} = \frac{1}{1 + (q - q_{th})(b_0^{(3)} + b_1^{(3)} q)^2} \quad \text{above } \omega\pi \text{ threshold,}$$

$$\eta_B^{(3)} = 1 \quad \text{below } \omega\pi \text{ threshold.}$$

We still obtain $\eta_3{}^1$ inconsistent with other channels and in addition the above parametrization does not have the correct threshold behavior. This is an undesirable feature of our fit but cannot be avoided. A likely explanation is that the f wave is being used to fit non-π exchange background in that region and is not the true ππ f wave amplitude. If the extrapolation for some reason (either background or the effect of using linear instead of a higher-order polynomial extrapolation) gives values for the moments above 900 MeV

*As noted earlier, one may let the d wave become inelastic at somewhat higher mass (~980 MeV) without altering results significantly.

0 0 0 0 3 8 0 0 2 5 1

that are higher than the true physical moments, then the easiest way to correct for that failure is to introduce a purely imaginary f-wave amplitude, since such a term would give a positive contribution to all the moments. We must point out though that results obtained for the p and s wave are little affected by this complication.* As long as we believe that the rapidly varying features in our data are due to the behavior of these waves (s and p), while the other waves are fairly smooth, the values obtained for s and p waves cannot change by much regardless of how the other waves are parametrized. This indeed was observed for the different fits attempted. We therefore feel confident that the general features of the I = 0 s wave and I = 1 p wave between 550 and 1150 MeV have been well determined by our fit.†

With the parameters obtained from our fit we can compute the phases and inelasticities. These are tabulated in Table V and shown in Figs. 5 and 6 for case 1 (see Table II). We point out that the given errors are computed by standard propagation of error and reflect only the statistical errors; they do not reflect the inherent uncertainties in performing an extrapolation. They should be considered only as an indication of the minimum error in our computed values. How accurate our results really are can only be ascertained by comparison with results of an experiment at different energy with comparable statistics.

For the p-wave phase shift (δ_1^1) we obtain the well-known Breit-Wigner shape (with $\delta_1^1 = 90°$ at 0.772 GeV, $\delta_1^1 = 45°$ at 0.703 GeV, and $\delta_1^1 = 135°$ at 0.863 GeV), the inelasticity (η_1^1) is close to unity within errors, although by 1.13 GeV it could be as small as 0.8. The I = 0 d-wave phase shift (δ_2^0) around 1 GeV is larger than what we would expect for the f_0 meson alone. This wave also seems to be quite inelastic ($\eta_2^0 \approx 0.80$ at 1.070 GeV). This result has to be viewed with caution because it depends strongly on what is assumed for the f-wave inelasticity, and non-π exchange background may have a substantial effect on these waves. The effect of the I = 2 d wave (δ_2^2) is small; we can obtain a good fit by setting $\delta_2^2 = 0$ throughout. The f-wave phase shift is small and negative under the ρ and becomes positive past the $\omega\pi$ threshold. As indicated before, the obtained inelasticity is too small to be compatible with the data in the inelastic channels; we believe that it is simply acting as a parametrization of background (or a failure of the extrapolation).

---

*This statement should be qualified somewhat for the p-wave inelasticity, which can change at high masses (1100 MeV) by as much as one standard deviation.

†Although computed errors are small on the p-wave phase, there might be a systematic error introduced by the effect (possible ρ-ω interference) between 760 and 800 MeV.

Table V. Phases and inelasticities (case 1).

Mass (GeV)	δ_0^0	η_0^0	δ_1^1	η_1^1	δ_2^0	η_2^0	δ_3^1	η_3^1
0.55	44 ± 2		9.4 ± 0.7		0 ± 0.5		0 ± 0.1	
0.625	57 ± 3		19 ± 0.8		0 ± 0.5		-0.4 ± 0.2	
0.665	64 ± 4		30 ± 1		0 ± 0.5		-0.5 ± 0.2	
0.690	68 ± 4		39 ± 1		0 ± 0.5		-0.6 ± 0.3	
0.71	71 ± 4		48 ± 1		0 ± 0.5		-0.8 ± 0.4	
0.73	74 ± 4		60 ± 1.5		0 ± 0.5		-0.8 ± 0.4	
0.745	76 ± 4		71 ± 1.5		0 ± 0.5		-0.9 ± 0.4	
0.755	77 ± 4		78 ± 1.6		0 ± 0.5		-0.9 ± 0.4	
0.765	78 ± 4		85 ± 1.6		0 ± 0.5		-0.9 ± 0.4	
0.775	79 ± 4		92 ± 1.6		0 ± 0.5		-1.0 ± 0.4	
0.785	80 ± 4		99 ± 1.5		0 ± 0.5		-1.0 ± 0.4	
0.795	81 ± 4		105 ± 1.5		0 ± 0.5		-1.0 ± 0.4	
0.810	82 ± 4		114 ± 1.4		1 ± 1		-1.1 ± 0.5	
0.83	84 ± 4		123 ± 1.2		1.5 ± 0.9		-1.1 ± 0.5	
0.85	86 ± 3.5		130 ± 1.1		2.0 ± 1		-1.1 ± 0.5	
0.87	88 ± 4		136 ± 1		2.7 ± 1		-1.1 ± 0.5	
0.89	91 ± 4		141 ± 0.8		3.5 ± 1		-1.1 ± 0.5	
0.91	96 ± 4		145 ± 0.8		4.4 ± 1		-1.0 ± 0.5	0.96 ± 0.02
0.935	107 ± 5		149 ± 0.9	0.99 ± 0.01	5.8 ± 1.2	0.99 ± 0.01	-0.8 ± 0.5	0.85 ± 0.05
0.965	134 ± 5.5		153 ± 1	0.99 ± 0.01	7.8 ± 1.4	0.99 ± 0.01	-0.5 ± 0.6	0.78 ± 0.05

(cont.)

Table V. (cont.)

Mass (GeV)	δ_0^0	η_0^0	δ_1^1	η_1^1	δ_2^0	η_2^0	δ_3^1	η_3^1
1.0	189 ± 9	0.62 ± 0.08	156 ± 1.2	0.98 ± 0.01	11 ± 2	0.95 ± 0.03	0.1 ± 0.8	0.74 ± 0.05
1.04	202 ± 9	0.54 ± 0.04	158 ± 1.6	0.96 ± 0.03	16 ± 2.5	0.88 ± 0.06	1.3 ± 0.7	0.72 ± 0.05
1.075	202 ± 8	0.58 ± 0.04	158 ± 2.5	0.94 ± 0.05	22 ± 4	0.85 ± 0.08	2.3 ± 0.8	0.72 ± 0.05
1.105	202 ± 8	0.63 ± 0.04	157 ± 3.4	0.92 ± 0.06	27 ± 4	0.89 ± 0.06	3.1 ± 1.1	0.74 ± 0.06
1.135	200 ± 8	0.69 ± 0.04	155 ± 4	0.92 ± 0.06	32 ± 5	0.96 ± 0.04	3.9 ± 1.8	0.76 ± 0.07
1.150	199 ± 7	0.70 ± 0.04	153 ± 6	0.92 ± 0.07	36 ± 7	0.96 ± 0.04	4.5 ± 2.0	0.78 ± 0.1

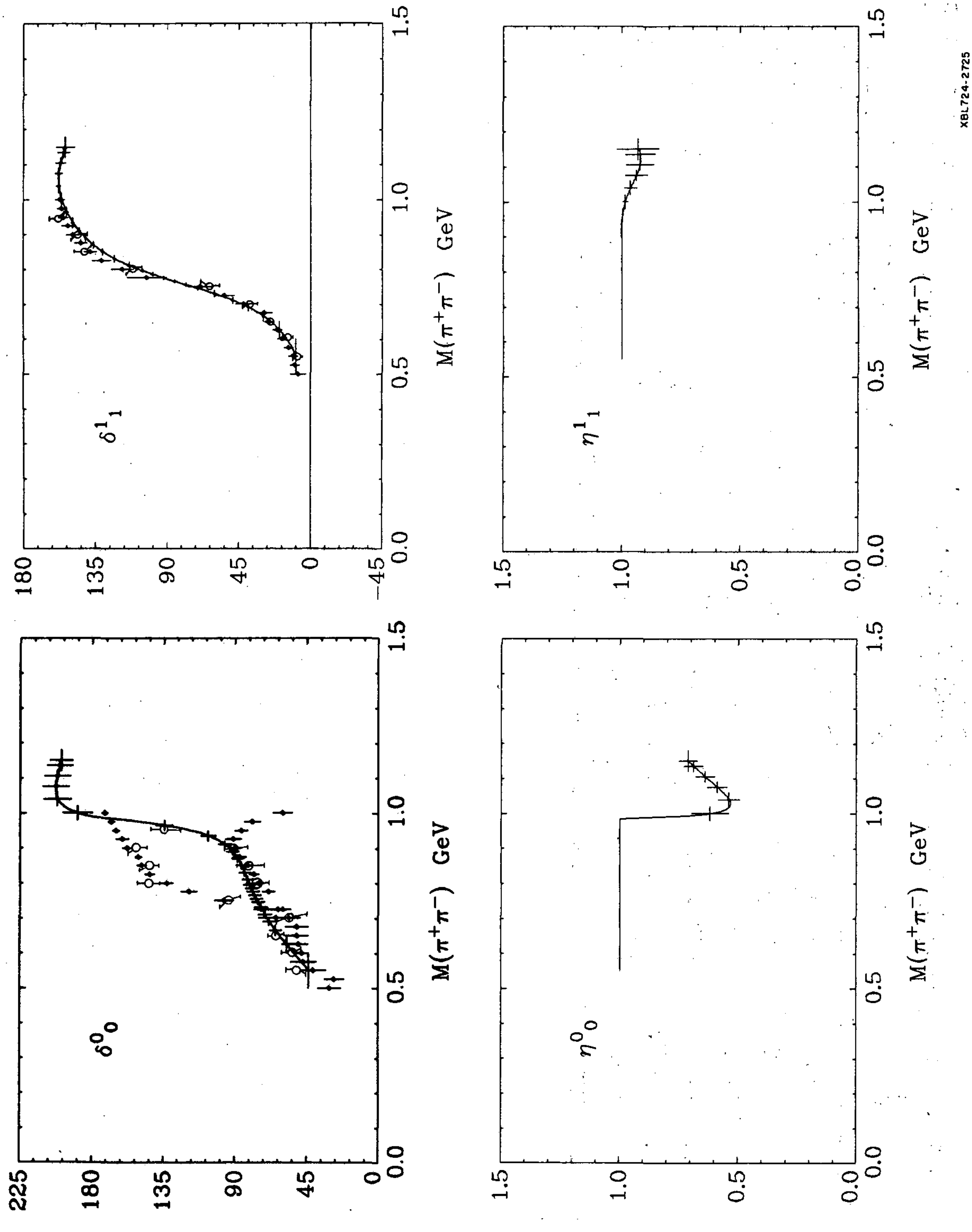

Fig. 5. Phases and inelasticities of I=0 s wave and I=1 p wave. The horizontal lines give size of bins used in fit. The vertical lines indicate the calculated errors at a given mass. These errors are purely statistical and do not reflect possible systematic effects introduced by the extrapolation procedure. The plotted points correspond to the elastic "down" and "up" solutions of Baton, Laurens, and Reignier.[23] The open circles correspond to the recent results of Baillon et al.[24]

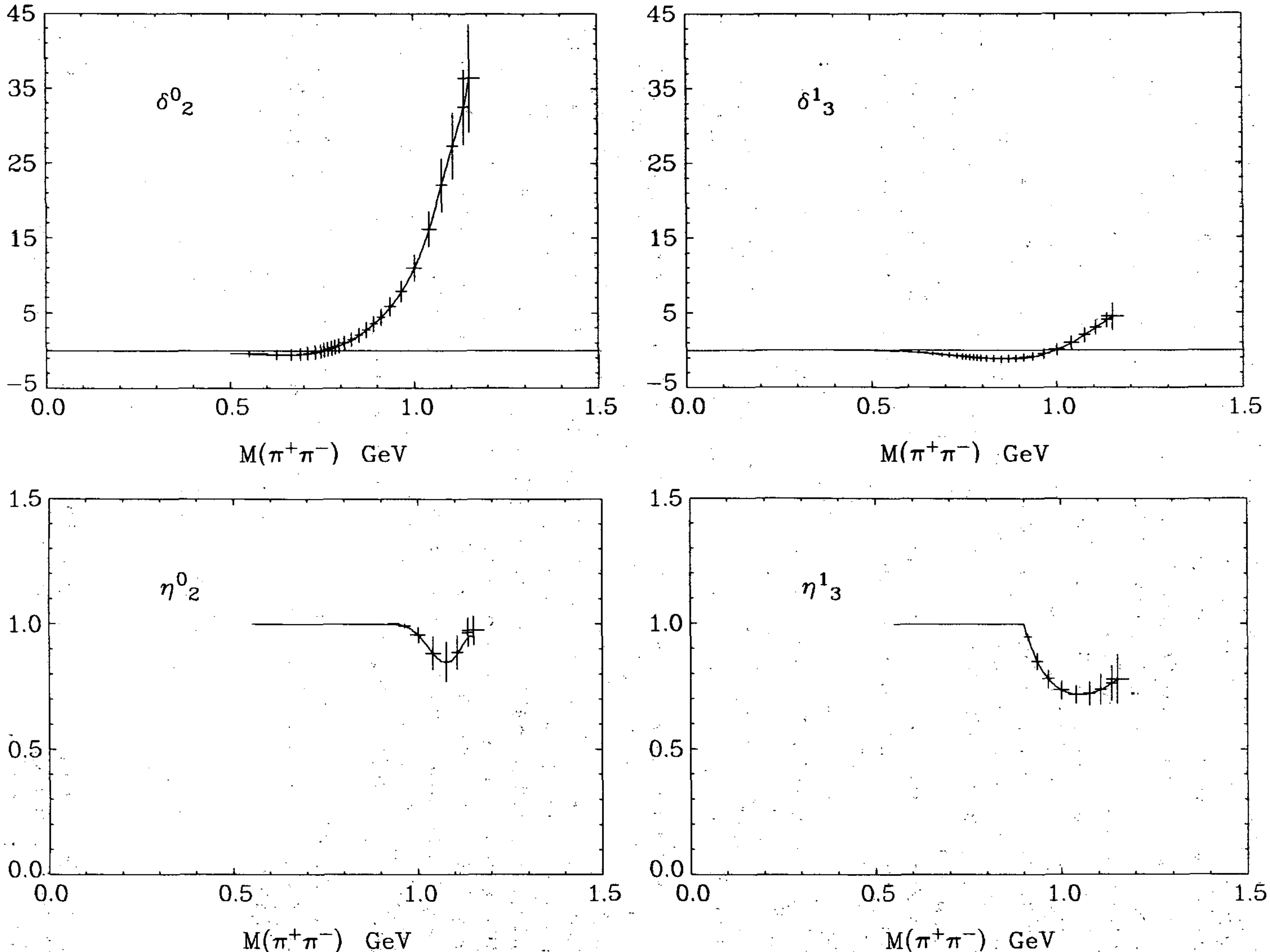

XBL724-2724

Fig. 6. Phases and inelasticities of I = 0 d wave and I = 1 f wave.

The most interesting results are the phase shift and inelasticity of the $I=0$ s wave. The phase rises from 45° at 550 MeV to 75° at 740 MeV, then increases slowly until 950 MeV, crossing 90° around 900 MeV. The phase below 850 MeV is in very good agreement with the one favored by Morgan and Shaw[17] (referred to as "between-down" solution). Above 900 MeV it increases rapidly, reaching 180° close to the $K\bar{K}$ threshold. Past the $K\bar{K}$ threshold the inelasticity reaches a minimum very rapidly (within 20 MeV), and then both phase and inelasticity vary rather slowly. At this point we should remark that the structure in the $\pi\pi$ data requires the maximum contribution of the s wave to the $K\bar{K}$ cross section to occur within 30 MeV of the $K\bar{K}$ threshold. This is consistent with our K^+K^- cross section ($|t'_{p\Delta}| < 0.1$ GeV^2) and the extrapolated cross section obtained by Hyams et al.[18] (in particular, the set "$t\sigma$" = bt and "$t\sigma$" = bt + ct^2), but is not consistent with the K^0K^0 cross section of Beusch et al.,[19] which reaches the maximum at 1.07 GeV. Part of the discrepancy might be from the fact that the Beusch et al. data are for $|t| < 0.5$ GeV, from differences in background for K^+K^- and K^0K^0, and from the mass difference between K^+ and K^0. This question deserves more careful study.

We can draw some interesting conclusions using our parametrization of the s-wave amplitude. We find that the amplitude T has two poles on the second Riemann sheet as a function of complex energy. One (S^*) is very close to $K\bar{K}$ threshold at $980 \pm 6 - i(37 \pm 8)$. The existence of a pole in this region was suggested from a K-matrix fit to the $K\bar{K}$ cross section by Hoang.[20] The other (ϵ) is quite far from the physical region, at $600 \pm 100 - i(250 \pm 70)$. Strictly speaking, we should say that there are four poles, since each one has a corresponding complex conjugate pole. Additional poles are also present, but these are quite far from the fitted region and no particular significance should be attached to them.

To check how dependent these results are on parametrization, we redid the fits with a somewhat different one (case 2 in Table II). In this case we added barrier factors to the $\ell \neq 0$ waves, i.e.:

$$\delta_B^{(\ell)} = qD_\ell(q) \sum_{n=0}^{N} a_n q^n,$$

where the $D_\ell(q)$ functions are defined in section IV [Eqs. (IV.9) and (IV.10)] and replaces $q^{2\ell}$ in Eq. (IV.6). For the M-matrix we took instead of Eq. (IV.12),

$$M_{ij} = M_{ij}^0 + M_{ij}^1 (E - E_0)$$

where E = c.m. energy, E_0 = E at $K\bar{K}$ threshhold. For M_{12} we added an extra term $M_{12}^2 (E - E_0)^3$. The best χ^2 with this parametrization was essentially the same (153.6 as compared with 152.2

for 147 degrees of freedom). The phases and inelasticities changed within the computed errors. We again obtain an S^* pole on the second Riemann sheet, at 975 ± 6-i (39 ± 8), but the ϵ pole is now on the fourth Riemann sheet at 650 ± 70-i (150 ± 50).† Note that for both of these poles a conventional Breit-Wigner parametrization will not be adequate: the ϵ is too far away from the real axis, and the S^* is too close to the $K\bar{K}$ threshold. We also computed the residues for these poles, which turn out to be complex. Finally, we can compute the $\pi\pi$ scattering length (case 1) for which we obtain $0.27 \pm 0.18\ \mu^{-1}$. The computation of the $\pi\pi$ scattering length of course assumes that our fit is valid down to the $\pi\pi$ threshold. Since we only fit down to 550 MeV the error should be considered to be much larger than the quoted one (which is purely statistical). This value agrees with the one obtained by Maung.[21] The $\pi\pi$ scattering length for case 2 turns out to be $-0.1 \pm 0.2\ \mu^{-1}$, which is 1 to standard deviation away from Maung value and more than 2 standard deviation away from the more recent results of Zylberstein et al.[22] These results are summarized on Table VI and Fig. 7.

Is our solution unique? We believe that the general features are unique—in particular, all the fits that we found with reasonable χ^2 exhibited the two poles in the s-wave amplitude. The situation for the other waves is less clear. In order to fit the moments we need substantial inelasticity in the d and f waves, less so in the p wave, although solutions with smaller $\eta_1{}^1$ than given by the selected fit could be obtained. Without more detailed information on the other channels one cannot choose among the various possibilities. In addition the amount of inelasticity needed in these waves is inconsistent with the number of events observed in the other channels. A possible explanation is that above 1 GeV the moments obtained by a linear extrapolation tend to be systematically higher than the true physical moments, maybe because of N^* background. Another possibility, although this seems less likely, is that the extrapolated $\omega\pi$ cross section is much larger than the one observed in $\pi^+ p \rightarrow \omega\pi^0 \Delta^{++}$ and the small inelasticities actually reflect very strong couplings for the reaction $\pi^+\pi^- \rightarrow \omega\pi^0$. Because of this complication and the lack of clear structure in the moments beyond 1150 MeV, we don't feel that the extrapolated data is sufficiently sensitive to warrant extending the analysis beyond this point.

VI. CONCLUSIONS

A coupled channel analysis ($\pi\pi$ and $K\bar{K}$) with a 2×2 M-matrix has yielded fruitful results on the $I = 0$ $\pi\pi \rightarrow \pi\pi$ s-wave scattering amplitude. The very marked structure of our data puts sufficient constraints to eliminate the "up-down" ambiguity, leaving the "down" solution as the only viable one between 750 and 950 MeV. Searching for poles in the complex energy plane, we found two of interest.

†On both sheets (II and IV), $\mathrm{Im}\, k_{\pi\pi}$ and $\mathrm{Im}\, k_{K\bar{K}}$ have opposite signs. On sheet II, $\mathrm{Im}\, k_{\pi\pi} < 0$; on sheet IV, $\mathrm{Im}\, k_{K\bar{K}} < 0$.

Table VI. Pole parameters for cases 1 and 2.

Case[a]	Pole position (MeV)	Residues[b] (units of π mass)	ππ scattering length
1	S^*		
	980 ± 5	$R_{11} \approx 0.052 - i0.062$	
	-i(37± 8)	$R_{12} \approx 0.087 + i0.035$	
	II sheet	$R_{22} \approx -0.007 + i0.110$	
	ϵ		
	600 ± 100	$R_{11} \approx -0.47 + i0.38$	0.27 ± 0.18
	-i(250±70)	$R_{12} \approx -0.36 + i0.27$	
	II sheet	$R_{22} \approx -0.28 + i0.21$	
2	S^*		
	975 ± 6	$R_{11} \approx 0.038 - i0.084$	
	-i(39±8)	$R_{12} \approx 0.087 + i0.072$	
	II sheet	$R_{22} \approx -0.116 + i0.08$	
	ϵ		
	650 ± 70	$R_{11} \approx 0.38 - i0.26$	-0.1 ± 0.2
	-i(150±50)	$R_{12} \approx 0.3 - i0.10$	
	IV sheet	$R_{22} \approx 0.22 - i0.02$	

[a] See Table II for an explanation of different cases.

[b] Residues defined as $R_{ij} = \frac{(s-s_0)}{\sqrt{q_i q_j}} T_{ij}(s_0)$, where $s_0 = s$ at pole position.

0 0 0 0 3 8 0 0 2 5 5

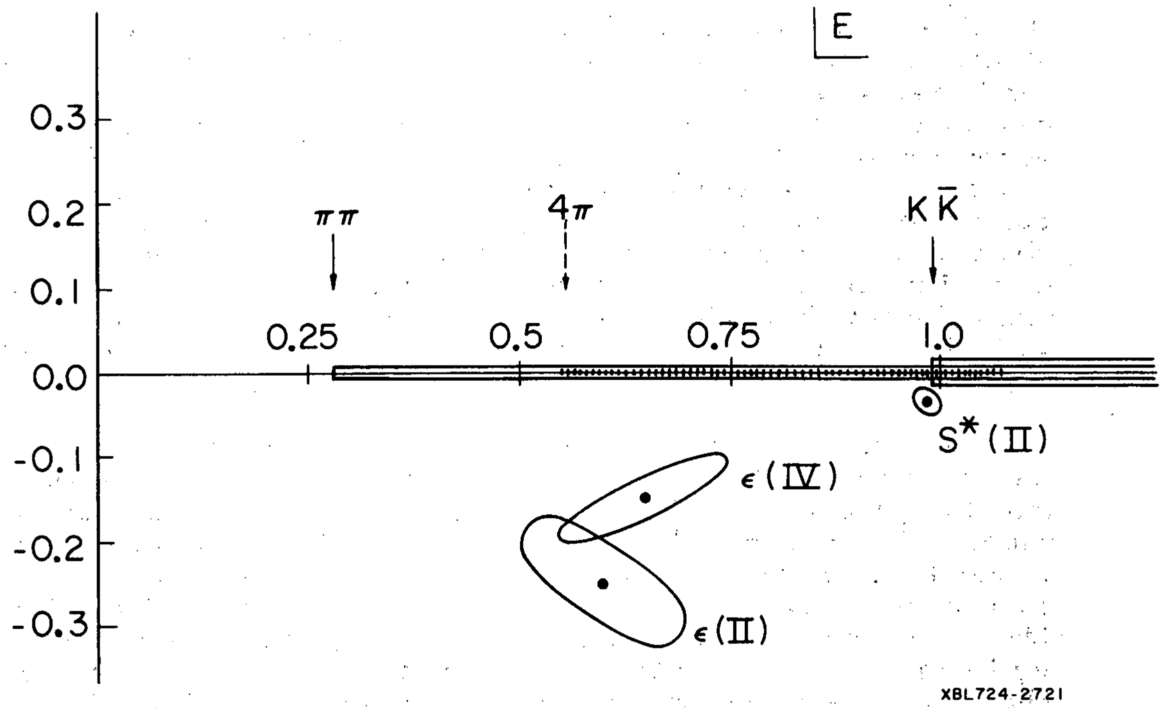

Fig. 7. Poles and cuts of the ππ s-wave amplitude in the complex energy plane. The dashes indicate region covered by our fit. Ellipses indicate (roughly) contours where χ^2 changes by one unit.

One (S^*), is very close to the $K\bar{K}$ threshold on the second Riemann sheet, at $980 \pm 7 - i\,(38 \pm 8)$. For the other ($\epsilon$) we found two possible locations, depending on the exact parametrization used. It could be either at $600 \pm 100 - i\,(250 \pm 70)$ on the second Riemann sheet, or at $650 \pm 70 - i\,(150 \pm 50)$ on the fourth Riemann sheet. Since for both cases the phases and inelasticities were not very different we conclude that considerably more data are needed to determine on which sheet it is. In addition, the effect of the 4π cut, which we neglect, might have to be taken into account. We also computed the $\pi\pi$ scattering length (this calculation implicity assumes that our fit is valid down to $\pi\pi$ threshold); we obtained $0.27 \pm 0.18\,\mu^{-1}$ (see Table VI).*

Because of background problems the results for the higher waves may have systematic errors. We obtain for the ρ mass (point at which $\delta_1^{\,1} = 90°$) 772 MeV and for its width (from points at which $\delta_1^{\,1} = 45°$ and $\delta_1^{\,1} = 135°$) 160 MeV. The width is somewhat larger than that found by other experiments.[1] This might be due in part to the effect (possibly ρ-ω interference) between 760 and 800 MeV. Beyond 1 GeV the data seem to require substantial inelasticity being inconsistent with the number of events observed in other channels. We believe this indicates that beyond 1 GeV the linear extrapolation tends to give $Y_L^{\,0}$ moments which are systematically higher than the true physical $Y_L^{\,0}$ moments.

ACKNOWLEDGMENT

We thank Prof. G. Chew, Dr. Gerard Smadja, and Dr. E. Colton for many useful discussions.

---

*After completing this work, we received a preprint by Y. Fujii, and M. Kato (University of Tokyo): "Effects of the $K\bar{K}$ threshold in $\pi\pi$ scattering." Using our previously published experimental results,[3] these authors reach conclusions rather similar to our own with quite a different method of analysis.

Addendum

At this conference several points were raised which could have some bearing on our results. P.K. Williams presented some model calculations on how absorption could affect the extrapolation of Y_L^0 moments. The main conclusion was that the effects are small ($< 10\%$) for $L \leq 3$, but can be quite substantial for $L = 4$ (25% or more) and are likely to be at least as large for $L > 4$.

Another point (raised by K.W. Lai) was the background in our K^+K^- events (e.g. ϕ production, or $C = -1$ events). Some crude estimates can be made by looking at our $\pi^+p \rightarrow \Delta^{++}K_sK_s$ ($C = +1$) and $\pi^+p \rightarrow \Delta^{++}K_sK_\ell$ ($C = -1$) events. There is no clear evidence for ϕ production when a Δ^{++} is selected with $|t'| < .1$ GeV^2. The Y_L^0 moments for K^+K^- events indicate that the amounts of $L \neq 0$ waves must be quite small below 1100 MeV. On the basis of a very small number of events with K_0K_0 mass < 1.1 GeV and $|t'| < .1$ GeV^2:

1) $\pi^+p \rightarrow \Delta^{++}K_0\overline{K}_0$ both K_0 decay in the chamber (18 events).

2) $\pi^+p \rightarrow \Delta^{++}K_0\overline{K}_0$ only one K_0 decays in the chamber (19 events),

We can conclude that, after correcting for various scanning and measuring inefficiencies, the above number of $K_0\overline{K}_0$ events is consistent with all K^+K^- events coming from S^* decay (within 15%).

We redid our case 1 fit assuming that the Y_L^0 ($L \geq 4$) moments are 30% smaller than the value obtained by a linear extrapolation. These corrections only affect the phase shifts above 900 MeV. The χ^2 for this fit is 118.0 for 147 degrees of freedom (CL = 96%). In Table VII we give the phase shifts obtained with the above corrections. We must emphasize that the corrections are quite uncertain and model dependent.

The main effect of this correction is to give more reasonable d and f waves. In particular the f-wave is much less inelastic, although the inelasticity is still a bit too small to be consistent with other channels. The s-wave phase shift is now somewhat larger above 1.0 GeV. The ϵ-pole is hardly affected, being at 604 - i 260 MeV (II sheet), while the S^* has become narrower, 986 - i32 MeV. Computed errors are of the same size as previously.

L. Gutay raised the point that if one looks at the isotropic term (IS) in the physical region it would seem to favor the up solution between 700 MeV and 880 MeV.* It is true that if one does an energy

---

* One can compute the isotropic term from the moments taking $IS = N(1 - \langle Y_2^0 \rangle / .252)$.

independent analysis it is difficult to rule out either solution in that region, the problem is compounded in our data between 760 MeV and 800 MeV where we cannot find any solution with an energy independent analysis because of $\rho-\omega$ interference. However, it is extremely unlikely that the "up" solution can be correct since it must join the down solution at 900 MeV where the data gives an unambiguous answer. Note (Fig. 5) that the two branches are well separated, so, if they join at some point they must do so within 20 MeV. In order to join, the phase shift will have to decrease by 40° or more within 20 MeV. From the Wigner condition of causality[25], $\frac{d\delta}{dq} > -R$, this would imply a radius of interaction of at least 15 fermi. The other possibility is that the phase shift goes through 180° before 900 MeV, which would imply that $\langle Y_1^0 \rangle$ is zero somewhere in that region, certainly not the case within our resolution ($\pm$ 5 MeV in the ρ - region). The errors on IS are too large to perform a meaningful extrapolation, however all information concerning this term is not lost since we extrapolate the normalized Y_L^0 moments and the cross section, from which one can calculate IS. Since our parametrization clearly fits all of them quite well, it cannot disagree with whatever term we chose to calculate from them. Using our phase shifts and the Chew-Low formula (III.2) we can compute IS in the physical region. In Fig. 8 we plot the isotropic term obtained from our data and the curves calculated with our solution alone and our solution plus 10% depolarization of the ρ. Although the fit is good, we have no other evidence that the ρ is depolarized by exactly 10%. The amount of depolarization depends sensitively on the detailed production mechanism. We see no compelling evidence for the claim that the "down" solution is in disagreement with the isotropic term.

A final comment concerns our case 2 solution. A more careful study of this particular parametrization reveals many undesirable properties which indicate that it should be rejected in favor of our case 1 solution. Although it reproduces the s-wave phase shifts in the fitted region, this solution has a pole on the I sheet at 680 - i 300 and another on the II sheet at 387 + i 40. The behaviour of the phase shift below 450 MeV is clearly pathological; it goes counterclockwise, being 180° at threshold instead of 0°.

Table VII. Phases and inelasticities after corrections.

Mass	δ_0^0	η_0^0	δ_1^1	η_1^1	δ_2^0	η_2^0	δ_3^1	η_3^1
.91	94 ± 4		145 ± .8		3.5 ± 1		-1. ± .5	.96 ± .02
.935	104 ± 5		150 ± .9	.99 ± .01	4.6 ± 1		-.5 ± .6	.89 ± .05
.965	133 ± 6		153 ± 1	.99 ± .01	6.0 ± 1.2	.99 ± .01	-.3 ± .7	.83 ± .05
1.0	192 ± 9	.61 ± .08	155 ± 1.2	.97 ± .01	8.8 ± 1.4	.96 ± .03	.1 ± .8	.80 ± .05
1.04	211 ± 9	.54 ± .04	155 ± 1.6	.93 ± .03	13. ± 2	.90 ± .06	1. ± .7	.79 ± .05
1.075	212 ± 8	.59 ± .04	154 ± 2.5	.89 ± .05	18. ± 3	.86 ± .08	2. ± .8	.80 ± .05
1.105	210 ± 8	.63 ± .04	152 ± 3.4	.87 ± .06	23 ± 4	.87 ± .06	3. ± 1.1	.81 ± .06
1.135	207 ± 8	.68 ± .04	150 ± 4	.86 ± .06	28. ± 5	.93 ± .04	4. ± 1.8	.84 ± .07
1.150	205 ± 7	.70 ± .04	150 ± 6	.85 ± .07	33. ± 7	.94 ± .04	4.5 ± 2.0	.88 ± .10

Table VIII. M-matrix parameter after corrections

$M^0_{11} = -3.03 \pm 2.2$	$M^0_{12} = 2.68 \pm .45$	$M^0_{22} = .028 \pm .4$
$M^1_{11} = -.444 \pm .70$	$M^1_{12} = .622 \pm .67$	$M^1_{22} = -.62 \pm .50$
	$M^2_{12} = .0023 \pm .0007$	

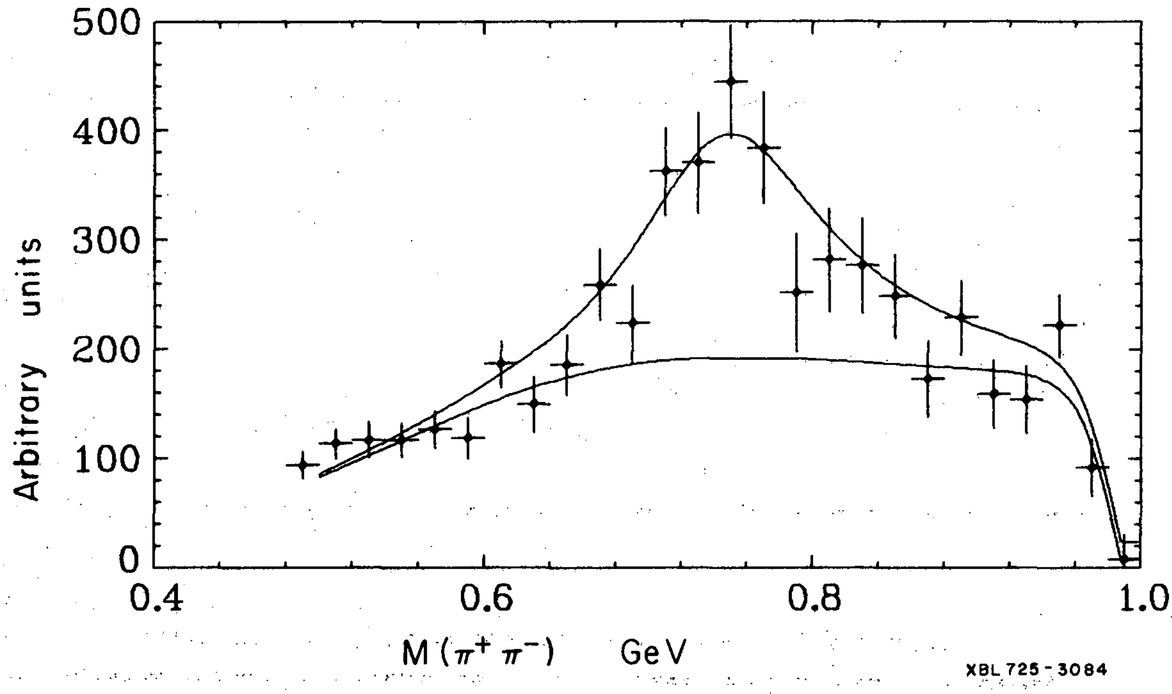

Fig. 8. Isotropic term for $|t' p\, \Delta| < .1$ GeV^2. The lower curve corresponds to the predicted s-wave contribution from our phase shift solution. The upper curve corresponds to s-wave plus 10% depolarization of the ρ-meson. Normalization is arbitrary, no attempt was made to optimize the fit.

REFERENCES

1. For a complete review of ππ scattering see:
Particle Data Group, Rev. Mod. Physics 43, S61 (1971).
D. Morgan and J. Pisut, Springer Tracts in Modern Physics 55 (1970).
J. L. Petersen, Physics Reports 2C, 157 (1971).

2. M. Alston-Garnjost et al., Phys. Letters 33B, 607 (1970).

3. M. Alston-Garnjost et al., Phys. Letters 36B, 152 (1971).

4. S. Flatté et al., Phys. Letters 38B, 232 (1972).

5. H. P. Dürr and H. Pilkuhn, Nuovo Cimento 40A, 899 (1965).

6. G. Wolf, Phys. Rev. Letters 19, 925 (1967).

7. E. Colton, P. Schlein, and E. Gellert, Physic Rev. D3, 1063 (1971); T. G. Trippe, Ph.D. thesis, UCLA-1026 (1968).

8. A. A. Carter et al., Nucl. Phys. B26, 445 (1971).

9. J. P. Baton, G. Laurens, and J. Reignier, Phys. Letters 33B, 528 (1970).

10. M. Gell-Mann, P. Sharp, and W. G. Wagner, Phys. Rev. Letters 8, 261 (1962).

11. C.J. Goebel and K.W. McVoy, Phys. Rev. 164, B1932 (1967).
L. Roper, R. Wright and B. T. Feld, Phys. Rev. 138, B190 (1965).

12. W. D. Walker et al., Phys. Rev. Letters 18, 630 (1967); J. P. Baton et al., ibid.; E. Colton et al., Phys. Rev. D3, 2028 (1967).

13. See for instance: J. P. Baton et al., ibid.; D. Morgan and J. Pisut, ibid.

14. For a description of M-matrix formalism and additional references see: A. Barbaro-Galtieri "Baryon Resonances," in Advances in Particle Physics, edited by R. L. Cool and R. E. Mashak (Wiley, N. Y., 1968). Vol. 2, 212.

15. P. H. Eberhard and W. O. Koellner, Lawrence Radiation Laboratory Report UCRL-20159 (1970).

16. E. Colton et al., Phys. Rev. D3, 2033 (1971).

17. D. Morgan and G. Shaw, Phys. Rev. D2, 520 (1970).

18. B. D. Hyams et al., in Experimental Meson Spectroscopy (Columbia University Press, N. Y., (1970), p. 41.

19. W. Beusch et al., ibid. p. 185.

20. F. T. Hoang, Nuovo Cimento 61A, 325 (1969).

21. T. Maung et al., Phys. Letters 33B, 521 (1970).

22. A. Zylberstein et al., Phys. Letters 38B, 457 (1972).

23. G. Laurens, Ph.D. thesis, University of Paris, CEA-N-1497, Table XI.

24. P. Baillon et al., Phys. Letters 38B, 555 (1972).

LEGAL NOTICE

This report was prepared as an account of work sponsored by the United States Government. Neither the United States nor the United States Atomic Energy Commission, nor any of their employees, nor any of their contractors, subcontractors, or their employees, makes any warranty, express or implied, or assumes any legal liability or responsibility for the accuracy, completeness or usefulness of any information, apparatus, product or process disclosed, or represents that its use would not infringe privately owned rights.

TECHNICAL INFORMATION DIVISION
LAWRENCE BERKELEY LABORATORY
UNIVERSITY OF CALIFORNIA
BERKELEY, CALIFORNIA 94720